

1-1-2008

Chemical synthesis and characterization of aniline based palladium composites and complexes

Jade Lorrayne Morgan
University of Nevada, Las Vegas

Follow this and additional works at: <https://digitalscholarship.unlv.edu/rtds>

Repository Citation

Morgan, Jade Lorrayne, "Chemical synthesis and characterization of aniline based palladium composites and complexes" (2008). *UNLV Retrospective Theses & Dissertations*. 2302.
<http://dx.doi.org/10.25669/su5f-7cmr>

This Thesis is protected by copyright and/or related rights. It has been brought to you by Digital Scholarship@UNLV with permission from the rights-holder(s). You are free to use this Thesis in any way that is permitted by the copyright and related rights legislation that applies to your use. For other uses you need to obtain permission from the rights-holder(s) directly, unless additional rights are indicated by a Creative Commons license in the record and/or on the work itself.

This Thesis has been accepted for inclusion in UNLV Retrospective Theses & Dissertations by an authorized administrator of Digital Scholarship@UNLV. For more information, please contact digitalscholarship@unlv.edu.

CHEMICAL SYNTHESIS AND CHARACTERIZATION OF ANILINE BASED
PALLADIUM COMPOSITES AND COMPLEXES

by

Jade Lorryne Morgan

Bachelor of Science
University of Nevada, Las Vegas
2005

A thesis submitted in partial fulfillment
of the requirements for the

Master of Science Degree in Chemistry
Department of Chemistry
College of Sciences

Graduate College
University of Nevada, Las Vegas
May 2008

UMI Number: 1456351

Copyright 2008 by
Morgan, Jade Lorrayne

All rights reserved.

INFORMATION TO USERS

The quality of this reproduction is dependent upon the quality of the copy submitted. Broken or indistinct print, colored or poor quality illustrations and photographs, print bleed-through, substandard margins, and improper alignment can adversely affect reproduction.

In the unlikely event that the author did not send a complete manuscript and there are missing pages, these will be noted. Also, if unauthorized copyright material had to be removed, a note will indicate the deletion.

UMI[®]

UMI Microform 1456351

Copyright 2008 by ProQuest LLC.

All rights reserved. This microform edition is protected against
unauthorized copying under Title 17, United States Code.

ProQuest LLC
789 E. Eisenhower Parkway
PO Box 1346
Ann Arbor, MI 48106-1346

Copyright by Jade Lorraine Morgan 2008
All Rights Reserved



Thesis Approval

The Graduate College
University of Nevada, Las Vegas

April 3, 2008

The Thesis prepared by

Jade L. Morgan

Entitled

Chemical Synthesis and Characterization of Aniline Based Palladium

Composites and Complexes

is approved in partial fulfillment of the requirements for the degree of

Master of Science

Examination Committee Chair

Dean of the Graduate College

Examination Committee Member
Examination Committee Member
Graduate College Faculty Representative

ABSTRACT

Chemical Synthesis and Characterization of Aniline Based Palladium Composites and Complexes

by

Jade L. Morgan

Dr. David W. Hatchett Examination Committee Chair
Associate Professor of Chemistry
University of Nevada, Las Vegas

The chemical synthesis of aniline based palladium materials was achieved by the use of the chemical oxidants, PdCl_4^{2-} and PdCl_6^{2-} . Complex formation was favored by using aniline and polymer formation was favored by the use of n-phenyl-1,4-phenylenediamine (NPPD). All materials were prepared with or without acid. Also, Characterization techniques such as FTIR spectroscopy, UV-Vis spectroscopy, Scanning Electron Microscopy, Thermogravimetric Analysis and X-ray Photoelectron Spectroscopy were used.

Hydrogen sorption studies were carried out using a GC/Hydrogen Generator. The aniline complexes had sorption properties up to 1.5% and the NPPD composites showed sorption up to 0.7%. It was found that the materials produced with PdCl_4^{2-} had higher sorption properties compared to the materials produced with PdCl_6^{2-} .

A separate study was performed using Sodium Borohydride to reduce palladium ions to metallic Pd in order to increase the rate and capacity of hydrogen sorption. Preliminary data showed the 0M HClO_4 Pd^{2+} complex to have 1.8% sorption compared to 1.5% before reduction.

TABLE OF CONTENTS

ABSTRACT.....	iii
LIST OF FIGURES	vi
ACKNOWLEDGMENTS	vii
CHAPTER 1 INTRODUCTION	1
1.1 Introduction to Conductive Polymers	1
1.2 Polyaniline	2
1.3 Polyaniline and Metal Composites	4
1.4 Applications	12
1.5 Research Approach	14
1.6 References.....	16
CHAPTER 2 EXPERIMENTAL	
2.1 Introduction.....	21
2.2 Materials	22
2.3 Instrumentation	22
2.4 References.....	28
CHAPTER 3 SYNTHESIS	
3.1 Synthesis of Polyaniline.....	29
3.2 Synthesis of Aniline/Palladium Materials	29
3.3 Synthesis of N-phenyl-1,4-phenylenediamine/Palladium Materials	38
3.4 Conclusion	45
3.5 References.....	46
CHAPTER 4 MATERIALS CHARACTERIZATION	
4.1 Introduction to Thermogravimetric Analysis.....	48
4.2 Scanning Electron Microscopy	55
4.3 Fourier-Transform Infrared Spectroscopy	63
4.4 X-ray Photoelectron Spectroscopy	68
4.5 Sodium Borohydride Reduction	71
4.6 Applications	77
4.7 Conclusion	83
4.8 References.....	85
CHAPTER 5 CONCLUSION	
5.1 Conclusion	87

VITA.....	89
-----------	----

LIST OF FIGURES

Figure 1.1	Polyaniline general form	2
Figure 1.2	Mechanism of formation of polymer units from aniline	3
Figure 2.1	General schematic of chemical synthesis	21
Figure 2.2	General GC run for hydrogen measurements	26
Figure 2.3	Calibration plot for hydrogen sorption measurements	27
Figure 3.1	Schematic of the reaction of aniline with palladium salts	30
Figure 3.2	UV-Vis spectra of filtrates from the reaction of K_2PdCl_4 with aniline	32
Figure 3.3	UV-Vis spectra of materials from the reaction of K_2PdCl_4 with aniline	33
Figure 3.4	UV-Vis spectra of filtrates from the reaction of K_2PdCl_6 with aniline	36
Figure 3.5	UV-Vis spectra of materials from the reaction of K_2PdCl_6 with aniline	37
Figure 3.6	Schematic of reaction of n-phenyl-1,4-phenylenediamine with Pd salts	38
Figure 3.7	UV-Vis spectra of filtrates from the reaction of K_2PdCl_4 with NPPD	40
Figure 3.8	UV-Vis spectra of materials from the reaction of K_2PdCl_4 with NPPD	41
Figure 3.9	UV-Vis spectra of filtrates from the reaction of K_2PdCl_6 with NPPD	43
Figure 3.10	UV-Vis spectra of materials from the reaction of K_2PdCl_6 with NPPD	44
Figure 4.1	Thermogravimetric graph of PANI, K_2PdCl_4 and K_2PdCl_6	49
Figure 4.2	TGA of aniline/palladium materials	51
Figure 4.3	TGA of NPPD/palladium materials	53
Figure 4.4	Image of crucible after thermal analysis	54
Figure 4.5	SEM image of pure PANI	55
Figure 4.6	SEM images of aniline/palladium complexes	58
Figure 4.7	SEM images of aniline/palladium complexes	59
Figure 4.8	SEM images of NPPD/palladium composites	61
Figure 4.9	SEM images of NPPD/palladium composites	62
Figure 4.10	FTIR of pure PANI	64
Figure 4.11	FTIR of aniline/palladium complexes	65
Figure 4.12	FTIR of NPPD/Palladium composites	67
Figure 4.13	XPS survey spectras	70
Figure 4.14	XPS of Pd 3d bands	71
Figure 4.15	FTIR spectra of PANI and $NaBH_4$ treated PANI	73
Figure 4.16	SEM images of $NaBH_4$ reduced aniline/ K_2PdCl_4 complexes	75
Figure 4.17	SEM images of $NaBH_4$ reduced aniline/ K_2PdCl_6 complexes	76
Figure 4.18	GC graph of aniline/0 M $HClO_4$ $PdCl_4^{2-}$	80
Figure 4.19	Hydrogen storage of aniline/palladium complexes	80
Figure 4.20	GC graph of NPPD/0 M $HClO_4$ $PdCl_4^{2-}$	82
Figure 4.21	Hydrogen storage of NPPD/palladium composites	82
Figure 4.22	Hydrogen storage of aniline/Pd complexes and $NaBH_4$ treated material ...	84

ACKNOWLEDGMENTS

It turns out that writing a thesis is a collective process from many people. My supporting cast came from all aspects of my life and without any one of them it is possible I may not be where I am today.

I would like to first and foremost acknowledge my advisor Dr. Dave Hatchett. He gave me a great opportunity to work in his lab when working quality control was not challenging enough. He was very understanding during the entire process. My committee members who had to sit and actually read my thesis, Dr. Dave Hatchett, Dr. Spencer Steinberg, Dr. Ken Czerwinski, and Dr. Jacimaria Batista, thank you, as well.

I work in a lab full of exceptional people. John Kinyanjui, Asanga Ranasinghe, and Nicole Millick all made this process easier by being available when I had no idea what I was doing (and when I needed to vent). I was fortunate to have two undergraduate students working under my direction. Emily Jensen and Whitney Shofner prepared countless samples, ran endless instruments and helped me tremendously.

I also had the help of other labs for acquiring pieces of data. I want to thank Dr. Das and Dr. Banerjee for the SEM images. Also, thanks to Dr. Clemens Heske, Dr. Marcus Bär, and Sujitra Pookpanratana for analyzing my materials on their XPS instrument. Kyle George and Lothar Weinhardt from Dr. Heske's group also helped towards the beginning of this project and I appreciate their time. I want to also thank them for the interesting time in their lab when I had to filter my solutions in a giant N₂ bubble. Kiel Holliday and Nick Smith helped me with some data that unfortunately I did

not use in this thesis. Nonetheless, they dedicated several hours of their time and I very much appreciated all their help. Lastly, I want to thank Dr. Spencer Steinberg for all his help with the hydrogen generator and GC. I was able to put those instruments out of commission a couple times and he fixed them with almost no witty remarks.

Finally, I would like to thank my family and friends. Even though I was missing in action for several months, I was fortunate to have a couple friends that checked up on me on many occasions. Their support helped me for the sole reason that I knew they were there and cheering me on. Last, but definitely not least, my mom. She gave me food, shelter and love and not necessarily in that order. She even let me get away with not doing the dishes and would feed my poor cat when I forgot.

This list could go on and on and I want to emphasize that. There were small things that certain people would do for me that made a huge impact on my day, week, or month. Thank you to everyone for watching me struggle through a difficult time and being there at the end.

CHAPTER 1

INTRODUCTION

1.1 Introduction to Conductive Polymers

The term molecular metal has been used to describe organic polymers that conduct electricity. Conducting polymers are becoming increasingly popular in research in the development of batteries¹, corrosion inhibitors^{2,3}, glass coatings for heat protection⁴ and composite materials with high tensile strength. These polymers are unique because their conductivities are similar to common metals. This class of polymers is termed intrinsically conducting polymers (ICPs) and they can be oxidized and reduced at generally low potentials with reversible redox behavior. Intrinsic conductive polymers are a class of polymers that achieve their conductivity through a process called doping. Doping is based on the uptake of charged species within the polymer matrix as a function of oxidation state. The dopant is responsible for the delocalization of charge throughout the polymer backbone enhancing conductivity.⁵ In polyaniline (PANI), the delocalized charge occurs through the proton doping of nitrogen in PANI allowing electrons to flow in the polymer.⁶ When ICPs are doped, the conductivities are typically $2\text{-}5\text{ S cm}^{-1}$, which is approximately 10 orders of magnitude greater than the undoped analog.⁷ Chemical doping of polymers can also influence the physical properties of the polymer. For example, anionic chemical doping can aid in increasing the polymers solubility.⁸

1.2 Polyaniline

Polyaniline (PANI) is the most extensively studied ICP. PANI is easy to synthesize both chemically and electrochemically, it is also environmentally stable and its chemical and electronic properties can be readily manipulated.^{9,10,11} A significant difference between PANI and other ICPs such as polythiophene or polypyrrole is that the polymer can be doped with protons and anions.^{12,13} Ion uptake in the polymer occurs for charge neutrality to be maintained.

Polyaniline (PANI) is synthesized from aniline using the chemical oxidant ammonium persulfate. It contains both oxidized and reduced units, which are represented in Figure 1.1, where the variable Y determines the concentrations each component. When $Y = 0.5$, it is referred to as the emeraldine base (EB) with equal units of benzenoid (reduced) and quinoid (oxidized) rings. When the emeraldine base is proton doped, it is called emeraldine salt and is the most conductive form of PANI.¹⁴ The balance of the benzenoid and quinoid units with proton doping of the amine/imine species increases the mobility of free charge carriers through delocalization of charge, which in turn increases the conductivity.¹⁵ Other forms of PANI that exist include the fully oxidized pernigraniline ($Y = 0$) and fully reduced leucoemeraldine ($Y = 1$). These forms of PANI are not conductive even with proton doping.^{16,17}

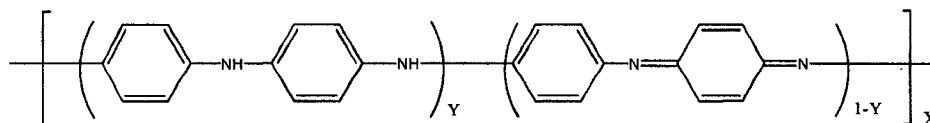


Figure 1.1. Polyaniline General Form.

1.2.1 Polyaniline Mechanism of Formation

Polymer initiation occurs through the initial oxidation of aniline to form the anilinium radical cation. The radical cation can then react with neutral aniline molecules. The loss of two protons produces the neutral species shown in Figure 1.2. This process is repeated multiple times to form long polymer chains. Polymer branching is minimized through preferential head to tail addition of each additional unit based on the resonance of the anilinium radical cation, which isolates the negative charge of the electron para to the nitrogen head group.

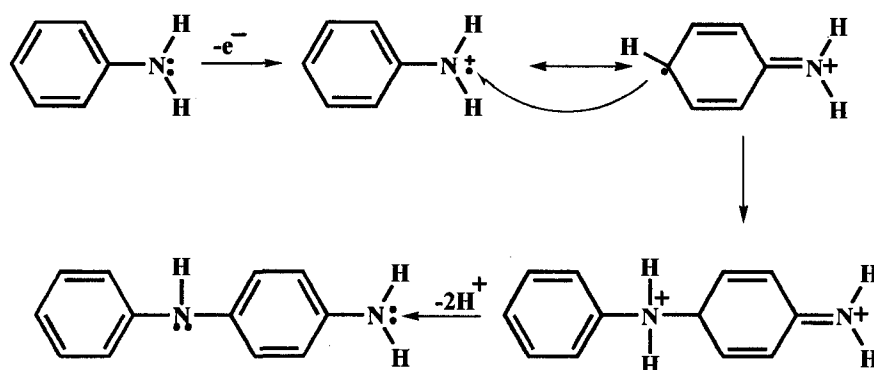


Figure 1.2. Mechanism of Formation of Polymer Units from Aniline.

The synthesis of PANI can be initiated using either chemical or electrochemical methods. Both methods produce the anilinium radical cation, which initiates polymerization. However, the synthetic processes are significantly different, producing materials with different properties and homogeneity. There are advantages and disadvantages for both methods that must be considered when considering the polymerization method. Typically, both electrochemical and chemical synthesis is

conducted in 1 M acid concentrations to promote proton doping and the conductivity of the material.

For the electrochemical synthesis of PANI, the applied potential is used to control both the rate and extent of the polymer reaction. The potential window can be monitored carefully to ensure that the polymer is not over oxidized, ensuring high homogeneity and the final oxidation state of the material produced.⁵ However, the amount of material produced using this method is limited and bulk quantities are not readily obtained. In addition, for the material to be used in other applications it must first be removed from the electrochemical interface compromising its properties. Cyclic voltammetry (CV) is the most common electrochemical method used to produce the polymer.³

Chemical synthesis methods allow bulk quantities of material to be produced rapidly through the direct chemical oxidation of aniline. Homogeneity of the material is low for chemical synthesis because the oxidation process cannot be controlled. Therefore, a range of oxidation states and molecular weights are obtained for the polymer. In addition, chemical synthesis of PANI can generate oligomeric products that are trapped in the bulk polymer that lower the inherent conductivity of PANI.¹⁸ The disadvantages of chemical synthesis are far outweighed by the ability to produce large quantities of polymer, which can be scaled easily to produce larger quantities.

1.3 Polyaniline and Metal Composites

The incorporation of metallic species in PANI is well documented and the materials produced have been referred to as a composite. Composites combine two species to obtain a mixed material, which may contain unique properties not observed in either individual component. PANI is a suitable material for the introduction of electron

deficient species because it contains high electron density and nitrogen heteroatoms with lone pair electrons that can be utilized for reduction reactions. In particular, transition metals such as Au, Pt, Ag, and Pd can be incorporated into PANI as ions and reduced to their metallic states. The polymer provides a stable matrix to disperse the metal species.¹⁹ Reduction of the oxidized metal species by the polymer compromises the conductivity as the polymer becomes more oxidized.¹⁵ However, in spite of the increased oxidation of the polymer, PANI/metal composites have been shown to be effective electrochemical catalysts. In addition, the PANI/metal composites have been utilized as transducers in chemical sensors, providing discrete reaction sites and metal-ligand reactions within the polymer matrix.²⁰

The synthesis of PANI/metal composites can be accomplished using the same methods described previously for the polymer alone. For the chemical synthesis, the key is the lone pair electrons on the nitrogen of aniline. Electron deficient metal anions can act as an oxidant when reacting with aniline producing the anilinium radical cation. The metal anion substitutes for the commonly used oxidant, ammonium persulfate in the polymerization reaction for PANI. The oxidation of aniline results in the reduction of the metal anion to form metal colloids in solution.¹⁵ These colloids are not protected and aggregate to form metal clusters. It has been suggested that the metal interacts with only the surface of the polymer forming larger clusters.²¹ For example, the spontaneous reduction of the metal species into preformed polymer reduction can only occur at the surface causing aggregation and cluster formation. However, when metal clusters form during the synthesis they provide nucleation sites for the polymer. In this manner, the clusters are dispersed as the polymer encapsulates the metal.^{19,22}

Regardless of the synthetic method, metal aggregation is an important factor because it influences the surface energy of the metal.²³ More recently, electrochemical methods have been utilized to evenly distribute the metal into the polymer by controlling the oxidation state and anion doping of PANI.^{20,24} In these studies, the metal ion was dispersed into the polymer during the normal anion doping at positive potential. Reduction of the metal anion is achieved as the potential is cycled to more negative potentials. This process can be repeated for additional dispersion and reduction of metal into the polymer. The oxidation of the metal was not observed after the reduction into the polymer matrix.²²

1.3.1 PANI/Au Composites

PANI/Au composite materials have been produced, extensively studied, and characterized.^{20,25,26} The chemical synthesis routes are varied throughout the literature because the synthetic parameters can be varied providing novel structural and chemically active materials. The materials can be produced with different morphologies, chemical and electronic properties.

For example, the oxidant AuCl_4^- solution was added dropwise to aniline prepared in acetic acid containing Tween 40.²⁵ The reaction was carried out in room temperature and a color change from clear to red was observed which was indicative of the formation of Au nanostructures. After further reaction, the solution turned green indicating the formation of PANI. These authors used XRD to examine the material, which produced diffraction patterns of Au metal. The product was PANI encapsulated Au, which the authors referred to as a core-shell particle. The authors also show that in the absence of

Tween 40, the uniformly coated PANI (400 nm)/Au particles (25 nm) did not form. The core-shell particles can be used for a variety of applications including catalysis.²⁷

Other methods have been developed for dispersion of the Au particles in PANI.¹⁹ For example, AuCl₃ has been dissolved in N-methylpyrrolidinone (NMP) and mixed with PANI (emeraldine base) in ratios ranging from 1:1 to 1:20 of Au:N in PANI. Initially, at lower concentrations the Au particles were not detected. However, after allowing the metal to react with the polymer for 40 minutes, metal deposits of < 4 nm was observed. At higher concentrations, the metal formed larger diameter deposits increasing with longer reaction times observed. XPS data suggested that the Au³⁺ was reduced to Au (0), with a corresponding increase in the =NH- as the metal was reduced and PANI was oxidized. Therefore, reduction of Au³⁺ occurred throughout the bulk of the material amine nitrogen.

A third approach was to combine the three components together at once; AuCl₄⁻, aniline, and the acid.²⁰ AuCl₄⁻ was used as the oxidizing agent for the formation of PANI as opposed to ammonium persulfate. The advantage of this study that the metal species is reduced during the polymer initialization step providing metal species for nucleation of the polymer. The synthesis provided a one pot synthesis of PANI/Au with evenly dispersed Au (1 μm diameter). The studies showed that the synthesis of PANI and reduction of Au did not reduce the conductivity of the polymer. The inherent conductivity of the polymer was maintained because the normal oxidative process for polymer formation was tied to the reduction and incorporation of the Au. In contrast, pre-formed polymer becomes more oxidized as a function of metal reduction.

1.3.2 PANI/TiO₂ Composites

Metal oxides such as TiO₂ can also be incorporated into PANI. Synthesis of PANI/TiO₂ from titanium isopropoxide in an acidic solution of HCl has been achieved. The colloidal TiO₂/acid was reacted with increasing volumes of neat aniline (0.3-1.0 mL) and sonicated to ensure thorough dispersion. Polymerization was then carried out by the dropwise addition of the oxidant, ammonium persulfate. A green precipitate was filtered indicative of the formation of PANI.²⁴ SEM analysis of the materials showed TiO₂ (8 nm diameter) encapsulated by the polymer. The conductivity of the PANI/TiO₂ material decreased by a factor of ten when compared to pure PANI in the emeraldine salt form. It is believed that these materials may be useful for catalysis, inclusion in solar cells, and for optoelectronic devices.²⁴

Sol-gel methods have also been used to prepare PANI/TiO₂ composite materials. Aniline was added to the metal solution, mixed and allowed to gel. Polymerization was then completed with the dropwise addition of ammonium persulfate to the gel. Imaging data shows that the polymer encapsulates TiO₂ at higher concentrations of the metal oxide. Lower concentrations of TiO₂ did not allow the sol-gel to form allowing the structure of PANI to be observed. SEM and elemental analysis indicated that as the percent weight percent of TiO₂ was increased, the size of the metal oxide increased. Interestingly, it was found that at low TiO₂ concentrations, the composites showed an increase in the conductivity compared to pure PANI.²⁸

1.3.3 PANI/Pt Composites

Platinum has known catalytic properties that when combined with the properties of PANI may prove useful.²⁹ Electrochemical and chemical synthesis of PANI/Pt

composites has been achieved. One chemical synthesis method proposed the use of K_2PtCl_6 or K_2PtCl_4 species as the chemical oxidant. However, the reaction of aniline with the two different Pt anions at different oxidation states did not produce the same materials. Only the reaction of PtCl_6^{2-} with aniline was shown to produce polymeric material with Pt metal. Reaction of PtCl_4^{2-} with aniline favored the formation of short chained oligomeric material rather than the polymer.²² Polymer was produced with PtCl_4^{2-} when n-phenyl-1,4-phenylenediamine was used rather than aniline as the polymer building block. The conductivity for all the PANI/Pd composites produced in these studies was low compared to pure PANI.

1.3.4 PANI/Ni and PANI/Sb Composites

The interest of these PANI/metal composites has progressed to other metals such as nickel (Ni) and antimony (Sb). For example, Ni^0 particles were synthesized through a reduction of $\text{Ni}(\text{OAc})_2$ in an organic medium of t-BuONa-activated NaH followed by the addition of aniline. The aniline displaces the t-BuONa from the surface of the Ni particles. Finally, oxidative polymerization was carried out by the dropwise addition of ammonium persulfate at room temperature to form the composite. The Ni diameter was measured after addition of various amounts of oxidant with the diameter increasing from 2.1 nm to 6 nm as the concentration was increased. The results indicate that the Ni^0 has a higher affinity for other Ni^0 surfaces aggregating while polymerization was progressing. XRD was used to examine the crystallinity of the Ni in amorphous PANI. The results demonstrated the first successful synthesis of PANI/ Ni^0 composites with an even distribution of the metal particles within the polymer matrix. In addition, the composites were stable with high reproducibility after catalytic Heck reactions were performed.³⁰

Similar methods have been used to introduce antimony into PANI. The semimetal is unique because it can exhibit high electron mobility when mixed with PANI. Introduction of either SbCl_3 or SbCl_5 into an organic solution of $t\text{-BuONa}$ at 65°C is followed by the addition of aniline.³¹ Aniline replaces the $t\text{-BuONa}$ protective group around the Sb particles. The oxidant ammonium persulfate was prepared in HCl and added dropwise to the aniline solution to produce the PANI/Sb composite. The oxidation state of the metal species influenced the final properties of the composite. The Sb^{3+} produced crystalline structures with diameters on the order of 10 nm. In contrast, the reduction of Sb^{5+} produced Sb with an average diameter of 2.0 nm. The solids formed from Sb^{5+} were found to have an uneven distribution of particles and random aggregation all through the polymer. The results of this study are preliminary in nature and highlight the interest of PANI/Sb with its anisotropic behavior and high electron mobility.

1.3.5 PANI/Pd Composites

The work presented in this thesis is focused on palladium metal. Pd has two oxidation states, Pd^{2+} and Pd^{4+} that can be utilized in chemical reactions. For example, the salts K_2PdCl_4 and K_2PdCl_6 provide PdCl_4^{2-} and PdCl_6^{2-} anions that are very similar to the Pt species used to produce the PANI/Pt composites. It is well documented that palladium metal reacts readily with nitrogen containing compounds making this metal an appropriate choice for producing PANI/Pd composites.^{32,33} However, PdCl_4^{2-} may react with aniline in the same manner as PtCl_4^{2-} producing oligomeric materials or a complex rather than the polymer. It has been shown that two derivatized aniline molecules can react with Pd^{2+} to form a metal/ligand complex with square-planar geometry.^{32,34}

Traditional chemical methods have been used to produce PANI/Pd composites. For example, aniline oxidation using ammonium persulfate in solutions containing PdCl_2 formed the composite.^{35,36} The polymer reduces Pd^{2+} to Pd^0 as it is formed. The diameter of the Pd^0 was consistent with the density of metal increasing with increasing concentration of Pd^{2+} . XPS data indicates that Pd^0 was deposited on the surface of PANI in polycrystalline form.³⁶

Synthesis of PANI/Pd composites in non-aqueous media has also been achieved.³⁷ The polymer was produced using aniline and ammonium persulfate using traditional synthetic methods. Solutions of palladium acetate, palladium acetylacetonate and PdCl_2 were prepared in acetonitrile and acetonitrile/acetic acid and mixed with the previously prepared PANI powder. A third solution was prepared containing PdCl_2 dissolved in NMP and then reacted with the polymer. The study demonstrates that the NMP/ PdCl_2 solutions had the highest reactivity with the polymer. In contrast, palladium acetylacetonate/acetonitrile solution did not react with the polymer at all. The study also demonstrated that solutions containing acetic acid incorporated predominately Pd^{2+} into the polymer rather than Pd^0 . The results indicate that Pd can exist as a chemical dopant (Pd^{2+}) or as a metal deposit (Pd^0) in PANI.

The chemical species and oxidation state of Pd ion strongly influences the final composition of the material. Therefore, the different solution conditions and methods have been examined in the literature to produce PANI/Pd composites. It was shown that there is no standard preparation method for the formation of the PANI/Pd composites. However, the synthesis of PANI using oxidized Pd species has not been presented in the literature. It is also noteworthy that no data was found on the preparation or analysis of

any composite using the Pd^{4+} species. It is expected that the oxidative strength of the Pd^{4+} ion will be greater than the Pd^{2+} ion. Pd^{4+} will produce a more oxidized polymer when reacted with the polymer, which is not typically desired. In contrast, the ability of Pd^{4+} ion to oxidize aniline is highly desired for polymer initiation.

The PANI/metal composite is unique because it combines the mechanical hardness and thermal stability of a metal with the structural diversity and variable electron density of the polymer.³⁸ In particular, PANI/Pd solids are efficient for the catalytic hydrogenation of alkenes and alkanes in comparison to PANI alone.³³ The PANI/Pd composites may also serve as a redox catalyst for oxidative reactions of primary alcohols in fuel cell applications.³⁹

1.4 Applications

PANI/Pd composites can influence redox reactions through normal catalytic mechanisms.³² The immobilization of the metal within the polymer matrix isolates the desired active sites by interaction with the nitrogen groups in the polymer, which can enhance catalytic activity through the minimization of poisoning.³⁶ The electron density of PANI is critical for the movement of electronic charge through the polymer backbone so that it can be localized at the metal active sites.⁴⁰ It has been previously determined that the amount of Pd^0 present in a system will directly increase the rate and efficiency of the reaction.^{36,39} This is likely tied to the active surface area of Pd that exists as the Pd^0 content increases. Oxidized forms of Pd are also possible and will directly influence the catalytic activity of the composites because Pd^{2+} does not necessarily induce catalytic activity. In addition, the reduction of Pd^{2+} to Pd^0 can cause the oxidation of PANI, decreasing the catalytic efficiency as the polymer becomes electron deficient.³⁶

Interestingly, acid concentration does not influence the reduction of Pd anions to Pd⁰. However, the incorporation of the Pd²⁺ ions into the polymer matrix is dependent upon the acid concentration because the Pd²⁺ anion will act as a dopant in the polymer in place of protons.⁴¹ In addition, comparison with other polymer/Pd models, such as poly(o-toluidine) and poly(chloroaniline), show lower palladium loading, demonstrating that PANI may be better suited for the integration and reduction to Pd metal particles.³⁷

Catalytic hydrogenation reactions are also possible with PANI/Pd composites. Reduction from terminal alkynes to cis-alkanes has been demonstrated with high selectivity.^{33,42} Pd-hydrides can be readily formed and will dissociate easily to produce active hydrogen atoms.⁴³ Palladium is known to be the most selective metal for the hydrogenation of dienes and acetylenes⁴² and Pd catalysts have also been shown to have potential in hydrodehalogenation in ground and wastewater.⁴⁴ Even though several studies have utilized Pd²⁺, none have attempted the use of Pd⁴⁺ with PANI.

PANI/Pd materials have also been utilized as transducers in chemical sensors. Uniform thin films of PANI can be produced and reacted with various species causing changes in the conductivity.⁴⁵ The change in conductivity is used to evaluate simple gas mixtures of O₂ and N₂. The PANI membranes can distinguish between the gases with a selectivity that far exceeds other known membranes.² PANI/Pd materials have been highly selective and sensitive methanol.^{38,46} In addition, the sensor showed structural and chemical stability after repetitive exposures to methanol. Other possible neutral organics, such as toluene and chloroform, do not alter the oxidation state of PANI, but influence the conductance through 'swelling' of the material.⁴⁷

PANI/Pd composites may also be useful in alternative energy applications.

Hydrogen as a power source for fuel cells and combustion engines has been proposed.⁴⁸ However, the storage is an issue and very few materials exist that can accommodate large amounts of hydrogen. Palladium is known for its hydrogen sorption characteristics to form hydrides.^{42,49} Highly dispersed Pd particles with small diameters will absorb higher concentrations of hydrogen when compared to bulk Pd surfaces.⁴⁹ The diameter is important because hydrogen sorption increases with increasing vacancy in the d-orbitals. Pd shows an increased vacancy in the 5d orbital when the size of Pd clusters is decreased.⁴⁹ Previous studies have shown that Pd can absorb 0.66 wt.% hydrogen at room temperature.^{43,50}

1.5 Research Approach

This thesis examines the use of PdCl_4^{2-} and PdCl_6^{2-} as the chemical oxidants in the synthesis of PANI/Pd composites. The influence of the oxidation states, Pd^{2+} and Pd^{4+} , are explored through reactions with aniline monomer and n-phenyl-1,4-phenylenediamine (NPPD), a two unit aniline species. There is no reference for the use of Pd^{4+} to produce PANI/Pd composites. The influence of the oxidation state of the metal anion on applications such as hydrogen storage properties will be examined. The use of PdCl_4^{2-} and PdCl_6^{2-} as the chemical oxidants is examined due to previous research showing that PtCl_4^{2-} and PtCl_6^{2-} do not always form polymer.^{18,51-56} There is some evidence that suggest that Pd(II) will preferentially form square planar complexes with aniline.³⁴ In addition, the influence of acid, HClO_4 , as a proton donor in this study is also explored to determine how acid doping influences the composition of the materials produced.

Characterization of the material produced was achieved using several instruments including; FTIR, UV-Vis, SEM and thermal analysis. Absorbance measurements were carried out using Fourier transform infrared spectroscopy (FTIR) and UV-Vis spectroscopy for evaluation of the organic component of the materials. These methods were used to probe the chemical properties of the materials to determine if polymer or complex formation occurs. Thermogravimetric analysis (TGA) was used to estimate the percent mass of Pd after thermal decomposition of the composites. This method does not distinguish between oxidized and reduced forms of Pd because Pd^{2+} and Pd^{4+} can be reduced as the polymer decomposes. X-ray diffraction spectroscopy (XRD) and X-ray photoelectron spectroscopy (XPS) were used to examine the structural and chemical characteristics of the metal and organic components, respectively. Scanning electron microscopy (SEM) was used to image the materials providing information at microscopic levels concerning the morphology of the materials. Finally, hydrogen sorption studies were performed using the thermal desorption GC/hydrogen sorption instrument to determine the hydrogen storage capacity of each material.

The ultimate goal of this research is the synthesis of viable PANI/Pd solids that will absorb and desorb hydrogen at low pressures without high thermal cycling. It has been suggested that HCl treated PANI may absorb 6-8 wt.%.⁵⁷ Other studies contradict these results with a mere 0.1 wt.% of hydrogen sorbed in the pristine polymer.⁵⁸ The addition of Pd with its known hydrogen sorption properties may enhance the sorption properties of the polymer. However, hydrogen sorption at PANI/Pd composites or complexes has not been previously examined.

1.6 References

- (1) Macdiarmid, A. G.; Yang, L. S.; Huang, W. S.; Humphrey, B. D. *Synthetic Metals* **1986**, *18*, 393-398.
- (2) MacDiarmid, A. G. *Synthetic Metals* **1997**, *84*, 27-34.
- (3) Stilwell, D. E.; Park, S.-M. *Journal of the Electrochemical Society* **1988**, *135*, 2491-2496.
- (4) MacDiarmid, A. G. *Synthetic Metals* **1986**, *21*, 79-83.
- (5) Syed, A. A. a. D., Maravattickal K. *Talanta* **1991**, *28*, 815-837.
- (6) Patil, A. O.; Heeger, A. J.; Wudl, F. *Chemical Reviews* **1988**, *88*, 183-200.
- (7) MacDiarmid, A. G.; Epstein, A. J. *Synthetic Metals* **1995**, *69*, 85-92.
- (8) Mantovani, G. L.; MacDiarmid, A. G.; Mattoso, L. H. C. *Synthetic Metals* **1997**, *84*, 73-74.
- (9) Wang, J.; Zhang, X.; Wang, Z. *Macromolecular Rapid Communications* **2007**, *28*, 84-87.
- (10) Xu, Y.; Dai, L.; Chen, J.; Gal, J. Y.; Wu, H. *European Polymer Journal* **2007**, *43*, 2072-2079.
- (11) Zhang, X.; Song, W. *Polymer* **2007**, *48*, 5473-5479.
- (12) Ginder, J. M.; Richter, A. F.; MacDiarmid, A. G.; Epstein, A. J. *Solid State Communications* **1987**, *63*, 97-101.
- (13) Chinn, D.; DuBow, J.; Li, J.; Janata, J.; Josowicz, M. *Chemistry of Materials* **1995**, *7*, 1510-1518.
- (14) Angelopoulos, M.; Dipietro, R.; Zheng, W. G.; MacDiarmid, A. G.; Epstein, A. J. *Synthetic Metals* **1997**, *84*, 35-39.

- (15) Kinyanjui, J. M.; Wijeratne, N. R.; Hanks, J.; Hatchett, D. W. *Electrochimica Acta* **2006**, *51*, 2825-2835.
- (16) Stejskal, J.; Kratochvíl, P.; Jenkins, A. D. *Polymer* **1996**, *37*, 367-369.
- (17) Hatchett, D. W.; Josowicz, M.; Janata, J. *Journal of Physical Chemistry B* **1999**, *103*, 10992-10998.
- (18) MacDiarmid, A. G.; Zhou, Y.; Feng, J. *Synthetic Metals* **1999**, *100*, 131-140.
- (19) Wang, J.; Neoh, K. G.; Kang, E. T. *Journal of Colloid and Interface Science* **2001**, *239*, 78-86.
- (20) Kinyanjui, J. M.; Hatchett, D. W.; Smith, J. A.; Josowicz, M. *Chemistry of Materials* **2004**, *16*, 3390-3398.
- (21) Tian, Z. Q.; Lian, Y. Z.; Wang, J. Q.; Wang, S. J.; Li, W. H. *Journal of Electroanalytical Chemistry* **1991**, *308*, 357-363.
- (22) Kinyanjui, J. M.; Harris-Burr, R.; Wagner, J. G.; Wijeratne, N. R.; Hatchett, D. W. *Macromolecules* **2004**, *37*, 8745-8753.
- (23) Smith, J. A.; Josowicz, M.; Engelhard, M.; Baer, D. R.; Janata, J. *Physical Chemistry Chemical Physics* **2005**, *7*, 3619-3625.
- (24) Dey, A.; De, S.; De, A.; De, S. K. *Nanotechnology* **2004**, *15*, 1277-1283.
- (25) Wang, Z.; Yuan, J.; Han, D.; Niu, L.; Ivaska, A. *Nanotechnology* **2007**, *18*.
- (26) Mallick, K.; Witcomb, M. J.; Scurrrell, M. S. *Journal of Materials Science* **2006**, *41*, 6189-6192.
- (27) Sun, S.; Murray, C. B.; Weller, D.; Folks, L.; Moser, A. *Science* **2000**, *287*, 1989-1992.

- (28) Xu, J. C.; Liu, W. M.; Li, H. L. *Materials Science and Engineering C* **2005**, *25*, 444-447.
- (29) Hasik, M.; Paluszkiewicz, C.; Bielańska, E. *Journal of Molecular Structure* **2005**, 744-747, 677-683.
- (30) Houdayer, A.; Schneider, R.; Billaud, D.; Ghanbaja, J.; Lambert, J. *Synthetic Metals* **2005**, *151*, 165-174.
- (31) Houdayer, A.; Schneider, R.; Billaud, D.; Lambert, J.; Ghanbaja, J. *Materials Letters* **2007**, *61*, 171-176.
- (32) Park, J. E.; Park, S. G.; Koukitu, A.; Hatozaki, O.; Oyama, N. *Synthetic Metals* **2004**, *141*, 265-269.
- (33) Drelinkiewicz, A.; Hasik, M.; Quillard, S.; Paluszkiewicz, C. *Journal of Molecular Structure* **1999**, *511-512*, 205-215.
- (34) Pan, Y. L.; Zhao, F.; Yang, S. *Acta Crystallographica Section E: Structure Reports Online* **2006**, *62*, m239-m240.
- (35) Drelinkiewicz, A.; Hasik, M.; Choczyński, M. *Materials Research Bulletin* **1998**, *33*, 739-762.
- (36) Drelinkiewicz, A.; Hasik, M.; Kloc, M. *Synthetic Metals* **1999**, *102*, 1307-1308.
- (37) Hasik, M.; Drelinkiewicz, A.; Wenda, E. *Synthetic Metals* **2001**, *119*, 335-336.
- (38) Mallick, K.; Witcomb, M.; Scurrall, M. *Platinum Metals Review* **2007**, *51*, 3-15.
- (39) Amaya, T.; Saio, D.; Hirao, T. *Tetrahedron Letters* **2007**, *48*, 2729-2732.
- (40) Houdayer, A.; Schneider, R.; Billaud, D.; Ghanbaja, J.; Lambert, J. *Applied Organometallic Chemistry* **2005**, *19*, 1239-1248.

- (41) Hasik, M.; Drelinkiewicz, A.; Wenda, E.; Paluszkiewicz, C.; Quillard, S. *Journal of Molecular Structure* **2001**, 596, 89-99.
- (42) Berger, F.; Varga, M.; Mulas, G.; Molnár, A.; Dékány, I. *Langmuir* **2003**, 19, 3692-3697.
- (43) Groszek, A. J.; Lalik, E.; Haber, J. *Applied Surface Science* **2005**, 252, 654-659.
- (44) Mackenzie, K.; Frenzel, H.; Kopinke, F. D. *Applied Catalysis B: Environmental* **2006**, 63, 161-167.
- (45) Virji, S.; Huang, J.; Kaner, R. B.; Weiller, B. H. *Nano Letters* **2004**, 4, 491-496.
- (46) Athawale, A. A.; Bhagwat, S. V.; Katre, P. P. *Sensors and Actuators, B: Chemical* **2006**, 114, 263-267.
- (47) Huang, J.; Virji, S.; Weiller, B. H.; Kaner, R. B. *Chemistry - A European Journal* **2004**, 10, 1314-1319.
- (48) Jurczyk, M. U.; Kumar, A.; Srinivasan, S.; Stefanakos, E. *International Journal of Hydrogen Energy* **2007**, 32, 1010-1015.
- (49) Huang, S. Y.; Huang, C. D.; Chang, B. T.; Yeh, C. T. *Journal of Physical Chemistry B* **2006**, 110, 21783-21787.
- (50) Ansón, A.; Lafuente, E.; Urriolabeitia, E.; Navarro, R.; Benito, A. M.; Maser, W. K.; Martínez, M. T. *Journal of Alloys and Compounds* **2007**, 436, 294-297.
- (51) Gawlicka-Chruszcz, A.; Stadnicka, K. *Acta Crystallographica Section C: Crystal Structure Communications* **2002**, 58, o416-o420.
- (52) Wei, Y.; Yu, Y. H.; Zhang, W. J.; Wang, C.; Jia, X. R.; Jansen, S. A. *Chinese Journal of Polymer Science (English Edition)* **2002**, 20, 105-118.
- (53) Rebourt, E.; Joule, J. A.; Monkman, A. P. *Synthetic Metals* **1997**, 84, 65-66.

- (54) Zhang, W. J.; Feng, J.; MacDiarmid, A. G.; Epstein, A. J. *Synthetic Metals* **1997**, *84*, 119-120.
- (55) Javadi, H. H. S.; Treat, S. P.; Ginder, J. M.; Wolf, J. F.; Epstein, A. J. *Journal of Physics and Chemistry of Solids* **1990**, *51*, 107.
- (56) Zhekova, H.; Tadjer, A.; Ivanova, A.; Petrova, J.; Gospodinova, N. *International Journal of Quantum Chemistry* **2007**, *107*, 1688-1706.
- (57) Cho, S. J.; Song, K. S.; Kim, J. W.; Kim, T. H.; Choo, K. In *ACS Division of Fuel Chemistry, Preprints*; 2 ed. 2002; Vol. 47, p 790-791.
- (58) Panella, B.; Kossykh, L.; Dettlaff-Weglikowska, U.; Hirscher, M.; Zerbi, G.; Roth, S. *Synthetic Metals* **2005**, *151*, 208-210.

CHAPTER 2

EXPERIMENTAL

2.1 Introduction

The chemical synthesis of polyaniline (PANI) was carried out using Pd^{2+} and Pd^{4+} as the chemical oxidant. The acid concentration was varied between 0M and 1.0M HClO_4 to determine the role of proton doping in the synthesis. Aniline and n-phenyl-1,4-phenylenediamine (NPPD) were used as the starting materials for PANI synthesis. From the schematic in Figure 2.1, a total of eight materials were produced.

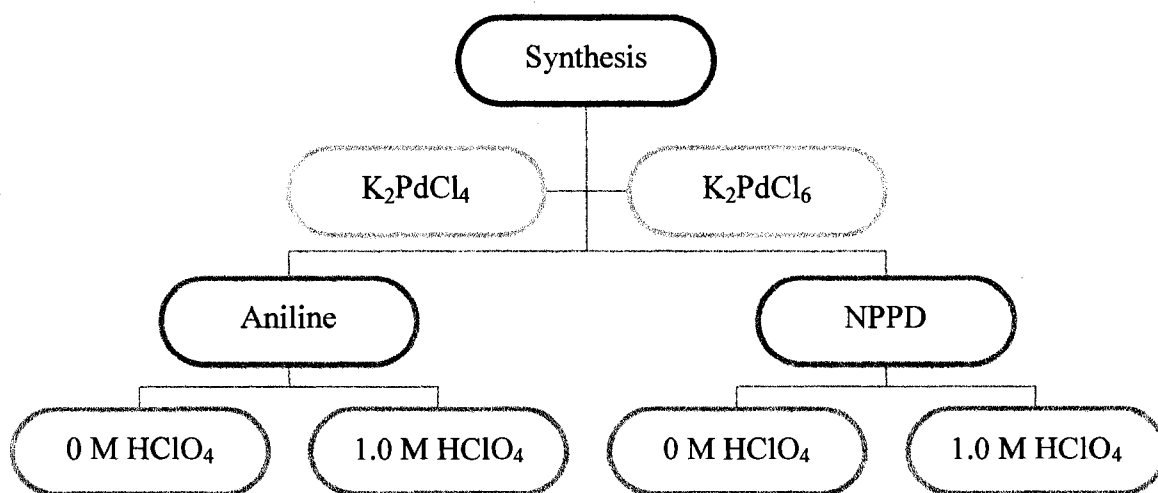


Figure 2.1: General schematic of chemical synthesis.

The characterization of the composites was achieved using several instruments. The composition of these solids was determined using Fourier transform infrared spectroscopy (FTIR), UV-Vis spectroscopy, and Thermogravimetric analysis (TGA). X-ray photoelectron spectroscopy (XPS) was used to determine oxidation state of palladium and the surface properties of the composites. Also, the composites were imaged using a scanning electron microscope (SEM) for surface morphological characteristics.

2.2 Materials

Perchloric acid, HClO_4 (Baker Analyzed, 69.0-72.0%, 7601-90-3), potassium hexachloropalladate, K_2PdCl_6 (Strem Chemicals, 99.0%, 93-4610), potassium tetrachloropalladate, K_2PdCl_4 (Strem Chemicals, 99.0%, 46-2126), n-phenyl-1,4-phenylenediamine (Aldrich, 98%, 05012MK), potassium bromide, KBr (PIKE technologies, 160-8010), ammonium persulfate, $(\text{NH}_4)_2\text{S}_2\text{O}_8$ (Mallinckrodt, 7277-54-0), Sodium Borohydride, NaBH_4 (Mallinckrodt, 98.0%, 16940-66-2), were used as received. Aniline, $\text{C}_6\text{H}_5\text{NH}_2$ (EM Science, 62-53-3) was distilled before use. All solutions were prepared with 18.3 $\text{M}\Omega\cdot\text{cm}$ water obtained from Barnstead E-pure water filtration system.

2.3 Instrumentation

FTIR Spectroscopy. All FTIR measurements were performed using a DIGILAB FTS-7000 spectrometer using a diffuse reflectance detector. All samples were mixed with KBr. Each sample was scanned 64 times with a resolution setting of 4 cm^{-1} and averaged to produce each spectrum. All samples were stored in a desiccator prior to measurements.

FTIR analysis was used to determine functional group composition of each material. The presence of polymer peaks is defined in the fingerprint region between

700-1600 cm^{-1} . The quinoid and benzenoid units can be identified in the FTIR spectrum of PANI at 1490 cm^{-1} and 1570 cm^{-1} , respectively. The C-N peak at 1295 cm^{-1} and the out-of-plane C-H peak at 821 cm^{-1} are also representative of PANI.¹ All materials produced using Pd species were compared to chemically pure PANI as a reference.

The oxidation state of PANI, as mentioned previously, is an important factor in the conductivity of the polymer. FTIR can be used quantitatively to determine the oxidation state of each material using a ratio of the benzenoid to quinoid peak area from the integrated quinoid and benzenoid from the IR spectra. The benzenoid peak represents the reduced units of the polymer and the quinoid peak represents the oxidized units.

Scanning Electron Microscopy (SEM). SEM images of all materials were obtained using a JEOL 4700 electron microscope equipped with a backscattered electron detector. Imaging was used to evaluate the morphological differences between the prepared materials. Samples were ground to provide a uniform coating on the carbon tape and the materials were gold coated to prevent charge interference. The differences between amorphous solids and polymer solids can be identified and the metal particles can appear as spherical aggregates.²

UV-Vis Spectroscopy (UV-Vis). Aqueous samples were analyzed using the StellarNet EPP2000 fiber optic UV-Vis spectrophotometer. This instrument is equipped with a D₂ lamp and tungsten filament source coupled into a single fiber. The signal is relayed to the detector after the transmitted light was passed through the cuvette. The integration time was ~100ms. All measurements were carried out in a 1 cm quartz cuvette with a Teflon cap. The filtrates from the prepared materials were also measured. Some dilution was required to keep the absorbance under two units. Solid samples were

dissolved in isopropyl alcohol and referenced against an isopropyl alcohol blank.

Polymer formation can be observed in the UV-Vis spectra at 380 nm region with oligomeric units around 400 nm.^{3,4} The incorporation of metal into the polymer matrix is also in the visible region of ~600nm.^{5,6}

Thermogravimetric Analysis (TGA). Thermal analysis was conducted using a Netzsch STA 449 C Thermal Analyzer. Samples were placed in alumina, Al₂O₃, crucibles. Thermal analysis was performed on all solid samples under air purge gas at a heating rate of 10° C/min. Each sample prepared was run on three separate batches and statistics were performed. Samples were stored in a desiccator prior to analysis. TGA was used to determine the percent mass of palladium in each sample. The total polymer/oligomer degradation content is obtained for each material at temperatures up to 1200°C. The polymer was vaporized leaving the Pd metal behind in the crucible providing an estimate of the % Pd in each sample.

X-ray Photoelectron Spectroscopy (XPS). Samples were left in solution and filtration was carried out in a nitrogen atmosphere to prevent the formation of oxides. Samples were transferred into the nitrogen-purged glove box that was connected to the load lock of the vacuum chamber. A rotary pump was then used to dry the samples prior to measurement. XPS analysis was measured on a Specs PHOIBOS 150MCD electron analyzer. Mg K α and Al K α excitation were used. The base pressure attained was in the 10⁻¹⁰ mbar range for all measurements. The electron spectrometer was calibrated according to literature⁷ using XPS and Auger line positions of different metals including Cu, Ag, and Au.

XPS measurements provide valuable information regarding the organic component and the oxidation state of the metal.

Hydrogen Generator/Thermal Desorption Gas Chromatograph (H₂/GC). The GC is a SRI 8610C gas chromatograph coupled with a hydrogen generator, which is a SRI H₂-50. The H₂ generator operates at approximately 32 psi and generates 50 mL/minute of hydrogen gas. Experiments on the GC were carried out on a porapak q column with a N₂ flow rate of 10mL/min. A porapak q column was used because hydrogen will not absorb on the column, while other materials from the decomposition of the sample will be retained. The GC column (porapak q) was set at a pressure of 20 psi and an isothermal temperature of 60°C. Materials were packed into a 2 mm x 200 mm thermal desorber column for analysis and contained by glass wool plugs on each end. The initial thermal desorber temperature was set at 35°C and the final temperature reached 200°C, at a rate of 1.5°C/second. All materials were purged with 30 psi H₂ for 90 seconds. The material was then exposed to a static pressure of 30 psi H₂ after the initial purge for various times; 5, 20, 40, 60, 90 minutes and up to 2 hours. During this time, operating parameters are held constant at a pressure of 20 psi and a temperature of 60°C. The run is started and heating is initialized at five minutes and switched off at nine minutes. The run ended after thirteen minutes in which time the thermal desorber column temperature returned to baseline (35°C).

Gas chromatograph studies were performed on each material to determine hydrogen sorption characteristics. Thermal desorption temperature was varied to determine each materials individual thermal threshold versus hydrogen storage capability. Figure 2.2 is representative of a general GC run and the peaks that are observed. The

unsorbed hydrogen will elute first because it is free of any physical or chemical bonds. The sorbed hydrogen elutes last, after a temperature increase, due to the interactions with the material. Figure 2.3 is the calibration curve performed on the GC instrument before analysis of the materials. Known volumes of hydrogen gas, from the hydrogen generator, were injected into the GC injection port and measured by the area under the peak.

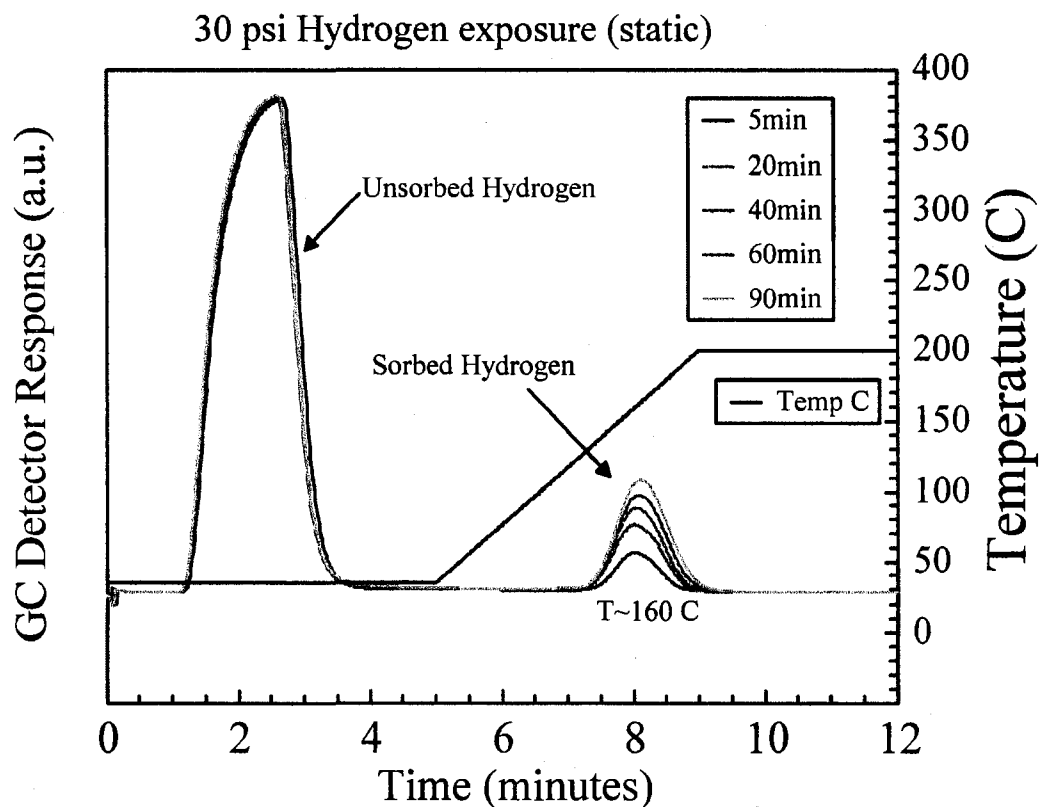


Figure 2.2 General GC run for hydrogen measurements. Temperature ramp begins at five minutes and ends at nine.

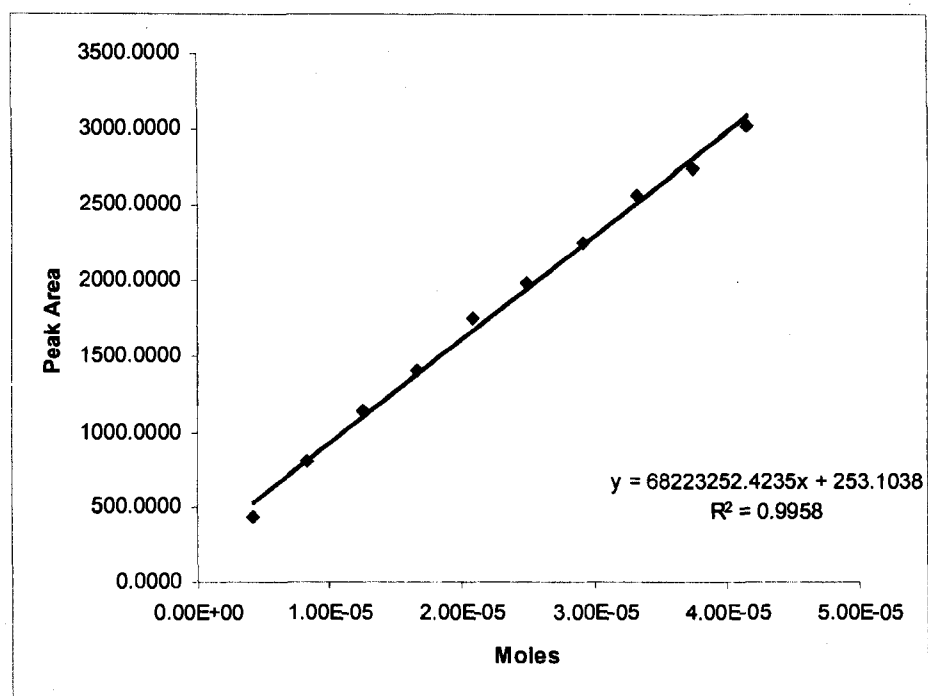


Figure 2.3 Calibration plot for hydrogen sorption measurements with moles versus peak area.

2.4 References

- (1) Hatchett, D. W.; Josowicz, M.; Janata, J. *Journal of Physical Chemistry B* **1999**, *103*, 10992-10998.
- (2) Kinyanjui, J. M.; Hatchett, D. W.; Smith, J. A.; Josowicz, M. *Chemistry of Materials* **2004**, *16*, 3390-3398.
- (3) Drelinkiewicz, A.; Hasik, M.; Choczyński, M. *Materials Research Bulletin* **1998**, *33*, 739-762.
- (4) Genies, E. M.; Boyle, A.; Lapkowski, M.; Tsintavis, C. *Synthetic Metals* **1990**, *36*, 139-182.
- (5) Mallick, K.; Witcomb, M. J.; Scurrrell, M. S. *Journal of Materials Science* **2006**, *41*, 6189-6192.
- (6) Park, J. E.; Park, S. G.; Koukitu, A.; Hatozaki, O.; Oyama, N. *Synthetic Metals* **2004**, *141*, 265-269.
- (7) Briggs, D. a. M. P. S.; Wiley: New York, 1990.

CHAPTER 3

SYNTHESIS

3.1 Synthesis of Polyaniline

The synthesis of pure PANI was prepared using ammonium persulfate, $(\text{NH}_4)_2\text{S}_2\text{O}_8$, as the chemical oxidant.¹⁻⁹ Two solutions were prepared as follows. In a 100mL volumetric flask, solution one contains 0.22 M of distilled aniline and 1M HClO_4 , in distilled H_2O . The second solution was 0.2 M $(\text{NH}_4)_2\text{S}_2\text{O}_8$ dissolved in a 100 mL volumetric flask in distilled H_2O . Solutions one and two were mixed together in a 250 mL erlenmeyer flask, allowed to react overnight, then vacuum filtered. PANI in the emeraldine salt form was obtained.^{3,9-14} It was then stored in the desiccator. The prepared PANI material was verified by FTIR spectroscopy.

3.2 Synthesis of Aniline/Palladium Solids

The synthesis of the aniline/Pd materials were carried out without $(\text{NH}_4)_2\text{S}_2\text{O}_8$ as the chemical oxidant. Either K_2PdCl_4 or K_2PdCl_6 was used in place as the oxidant for the synthesis. Figure 3.1 shows a schematic representation of the materials produced using the Pd anions. This approach has been successful in the production of PANI/Au composites. However, our materials are different colors, previously indicative of either chemical or oxidative differences in the products.¹⁵ The products had a range of colors and consistencies indicating that the synthesis produced different materials with different oxidation states.

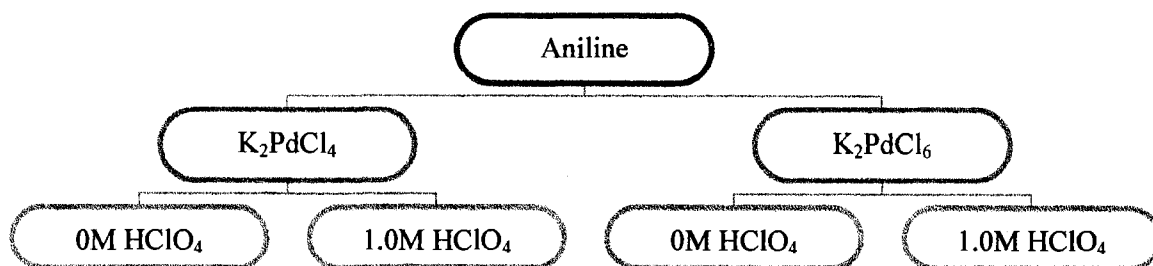


Figure 3.1: Schematic of the reaction of aniline with palladium salts.

3.2.1 Synthesis of Aniline/Pd²⁺ Materials

The synthesis of PANI/Pd²⁺ materials was achieved by mixing 50 mL of 2.02×10^{-2} M K₂PdCl₄ (Pd²⁺) with 1 mL of 0.22 M aniline in the presence and absence of acid (1 M HClO₄). The aniline was added in excess to ensure complete reaction. The final mole ratio of the aniline/metal was approximately 10:1. See Figure 3.1 for the schematic of the synthesis. The mixtures were left to react overnight. The product was vacuum filtered, washed with copious amount of water and stored in the desiccator.

Filtrates of both solutions were collected and analyzed by UV-Vis spectroscopy to evaluate the extent of the reaction of the Pd anion in Figure 3.2. Excess aniline was present in the filtrate solutions at ~250 nm. These results were found to be consistent after analysis of several reaction filtrates. The spectra also showed the disappearance of the PdCl₄²⁻, indicating that the filtered materials retained the bulk of the palladium.

UV-Vis spectroscopy was also used to analyze the materials. Aniline has a characteristic absorbance in the ultra violet region at 260 nm. The Pd salt has multiple bands between 220 and 340 nm and one distinct peak at 420 nm. The UV-Vis spectra in Figure 3.3 are different than the two starting materials. The bands for aniline and the Pd

salt are not observed for the products. The 0 M HClO₄ Pd²⁺ material has two peaks at 220 and 310 nm. The 1.0 M HClO₄ Pd²⁺ material also has two peaks, but shifted to 250 and 280 nm. PANI has a π - π^* transition between 320 and 360 nm and a polaron- π^* at 440 nm.¹⁶⁻¹⁸ The polaron- π transition from 650 to 750 nm should also be present. The absence of any and all of these peaks indicates that these particular materials are not highly incorporated into the materials as the salt.

Even though there are no indicative peaks for PANI formation, the results do not exclude oligomeric material formation. One group examined oligomers such as a tetramer and a 16-mer using UV-Vis to determine their optical signature.¹⁹ Their UV-Vis data suggested that smaller oligomers are shifted to lower wavelengths while characteristic PANI peaks are typically at much higher wavelengths. For example, the band associated with the polaron- π transition shifts from 638 nm to 590 nm for the tetramers of aniline. In addition, the lower bands at 200-400 nm can be attributed to lower molecular weight oligomers.¹⁵

The chemical synthesis of PANI/Pd²⁺ using aniline without acid produced a pale yellow material with an average yield of $0.3772 \text{ g} \pm 0.1145$ based on four synthetic trials. The material prepared in 1.0 M HClO₄ also had a pale yellow color, but had a different consistency in comparison to the first material. Average recovered yield for 1.0 M HClO₄ material was $0.3378 \text{ g} \pm 0.0152$ for four synthetic trials.

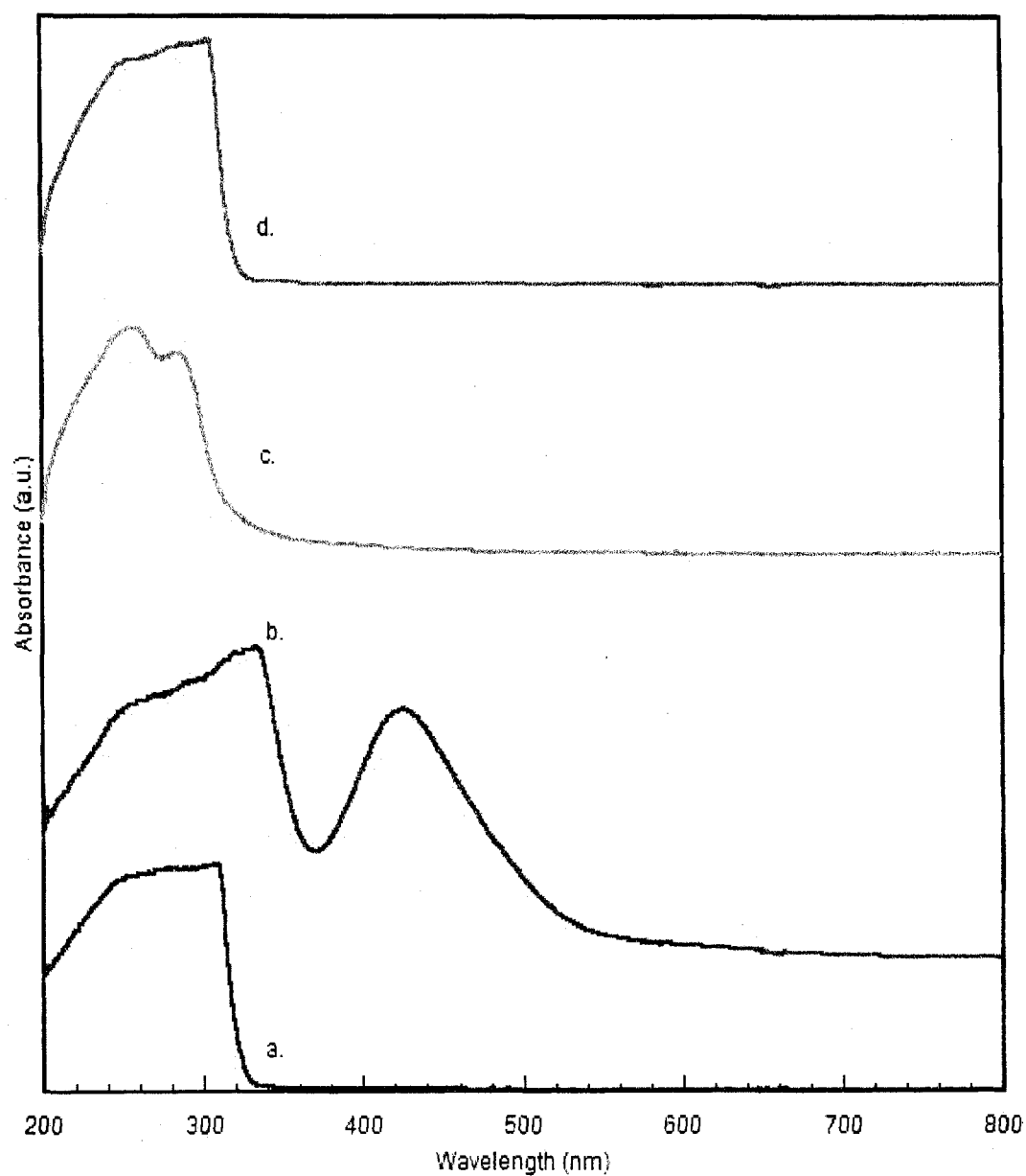


Figure 3.2: UV-Vis spectra of filtrates produced from the reaction of K_2PdCl_4 with Aniline. (a) Aniline (b) K_2PdCl_4 (c) Aniline/ $PdCl_4^{2-}$ material with 1.0 M $HClO_4$ (d) Aniline/ $PdCl_4^{2-}$ material with 0 M $HClO_4$

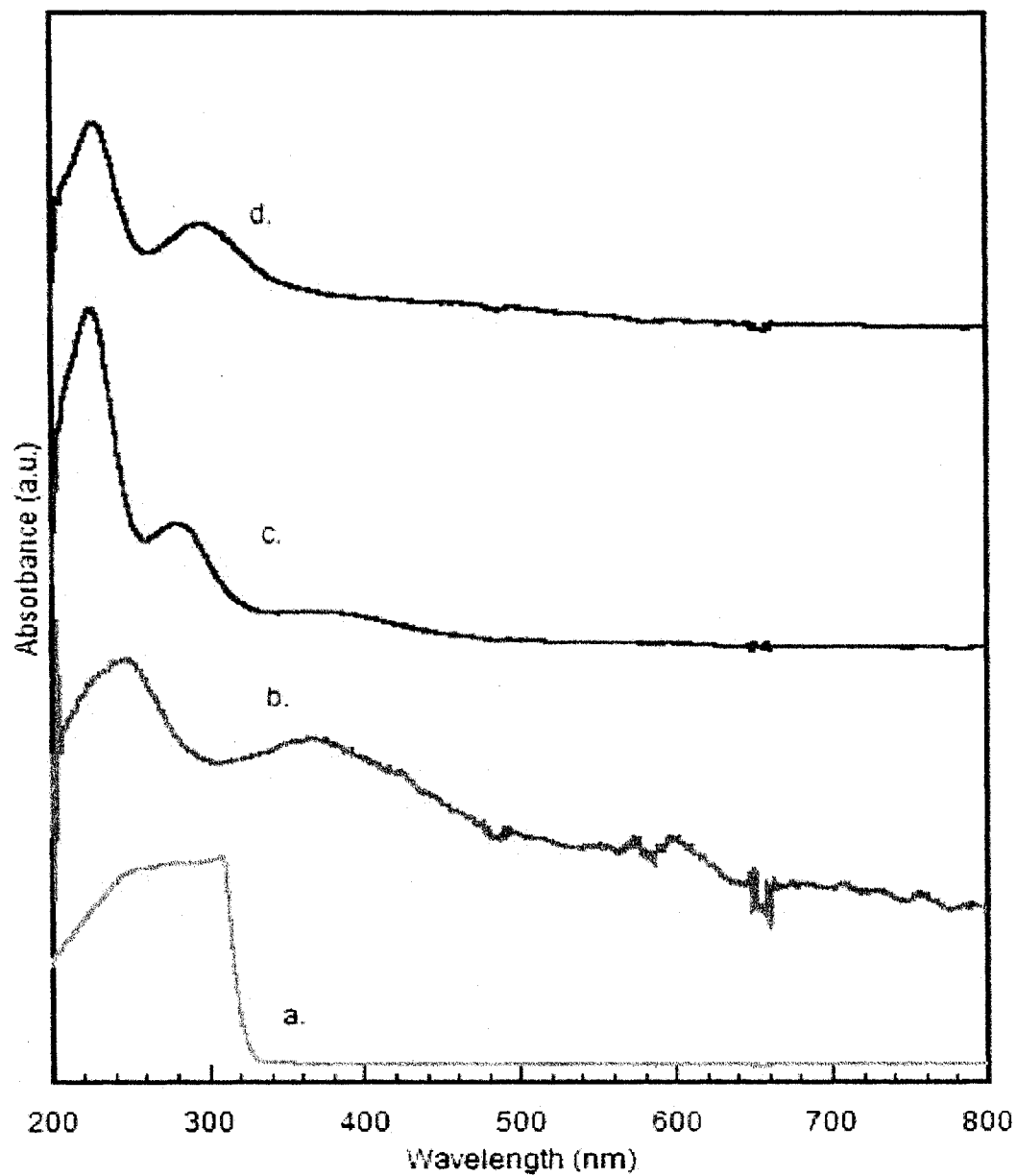


Figure 3.3: UV-Vis spectra of the materials produced from the reaction of K_2PdCl_4 with Aniline. (a) Aniline (b) K_2PdCl_4 (c) Aniline/ $PdCl_4^{2-}$ material with 1.0 M $HClO_4$ (d) Aniline/ $PdCl_4^{2-}$ material with 0 M $HClO_4$

3.2.2 Synthesis of Aniline/Pd⁴⁺ Solids

A similar synthetic route was used for the synthesis of aniline/PdCl₆²⁻ materials. The synthesis of PANI/Pd⁴⁺ materials was achieved by mixing 50 mL of 1.20 x 10⁻² M K₂PdCl₆ (Pd⁴⁺) with 1 mL of 0.22 M aniline in the presence and absence of acid (1 M HClO₄). The aniline was added in excess to ensure complete reaction. The final mole ratio of the aniline/metal was approximately 10:1. See Figure 3.1 for the schematic of the synthesis. Solutions were left to react overnight. The solutions were vacuum filtered, washed with copious amount of water and stored in the desiccator.

Filtrates of both solutions were collected and analyzed by UV-Vis spectroscopy to observe complete reduction of the starting materials and can be seen in Figure 3.4. Excess aniline was present in both filtrate solutions at ~250 nm. These results were found to be consistent after analysis of several reaction filtrates. The spectra also showed the disappearance of the PdCl₆²⁻ peaks, indicating that the filtered materials retained the palladium.

UV-Vis spectroscopy was also used to analyze the filtered materials and can be seen in Figure 3.5. The characteristic bands from the PdCl₆²⁻ salt are not present in the spectras of the materials with the exception of a small broad band at 400 nm in the 1.0 M HClO₄ Pd⁴⁺ spectrum. The presence of this peak may be related to a couple different species. First of all, it may be left over salt, even though this band is significantly diminished from the corresponding band in bulk. It is possible that there is unreacted PdCl₆²⁻ trapped in the material, which gives rise to the band. It may also be possible, that the small, broad band is indicative of polymer formation. As stated earlier, the π - π^* transition between 320 and 360 nm and the polaron- π^* at 440 nm represent PANI

formation. The lack of a band in the 600 nm region suggests that pure PANI may have formed, but the oxidation state is different than the emeraldine state. This data is difficult to analyze because the salt peaks are overlapping with characteristic PANI peaks. In the 0 M HClO₄ Pd⁴⁺ spectra, no broad peak is observed in the 400 nm region, suggesting the formation of complexes over polymer.

The 0 M HClO₄ Pd⁴⁺ material had an average yield of $0.1897 \text{ g} \pm 0.0142$ based on four synthetic trials. The material produced from 1.0 M HClO₄ Pd⁴⁺ had an average yield of $0.2150 \text{ g} \pm 0.0127$ based on four synthetic trials.

From the UV-Vis data it can be concluded that there are slight differences between the Pd²⁺ materials and the Pd⁴⁺ materials. It takes more electrons to reduce the metal from the Pd⁴⁺ oxidation state compared to the Pd²⁺ oxidation state therefore more likely to form more radical species that can be used to form longer chain structures of aniline in solution. Therefore, the Pd⁴⁺ materials produced have absorption characteristics consistent with small quantities of oligomer/polymer, while Pd²⁺ data is indicative of complex formation.

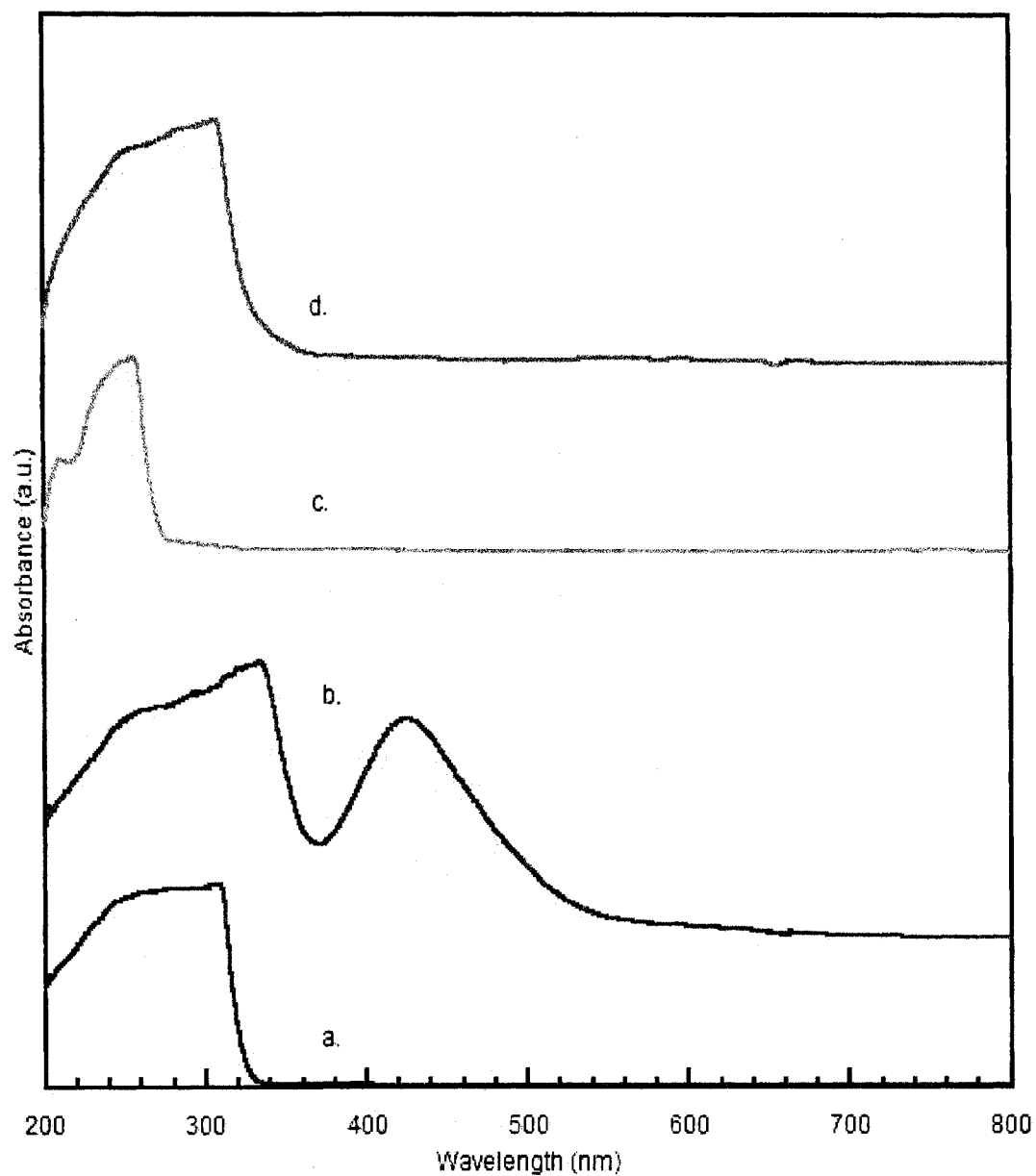


Figure 3.4: UV-Vis spectra of the filtrates produced from the reaction of K_2PdCl_6 with Aniline. (a) Aniline (b) K_2PdCl_6 (c) Aniline/ $PdCl_6^{2-}$ material with 1.0 M $HClO_4$ (d) Aniline/ $PdCl_6^{2-}$ material with 0 M $HClO_4$

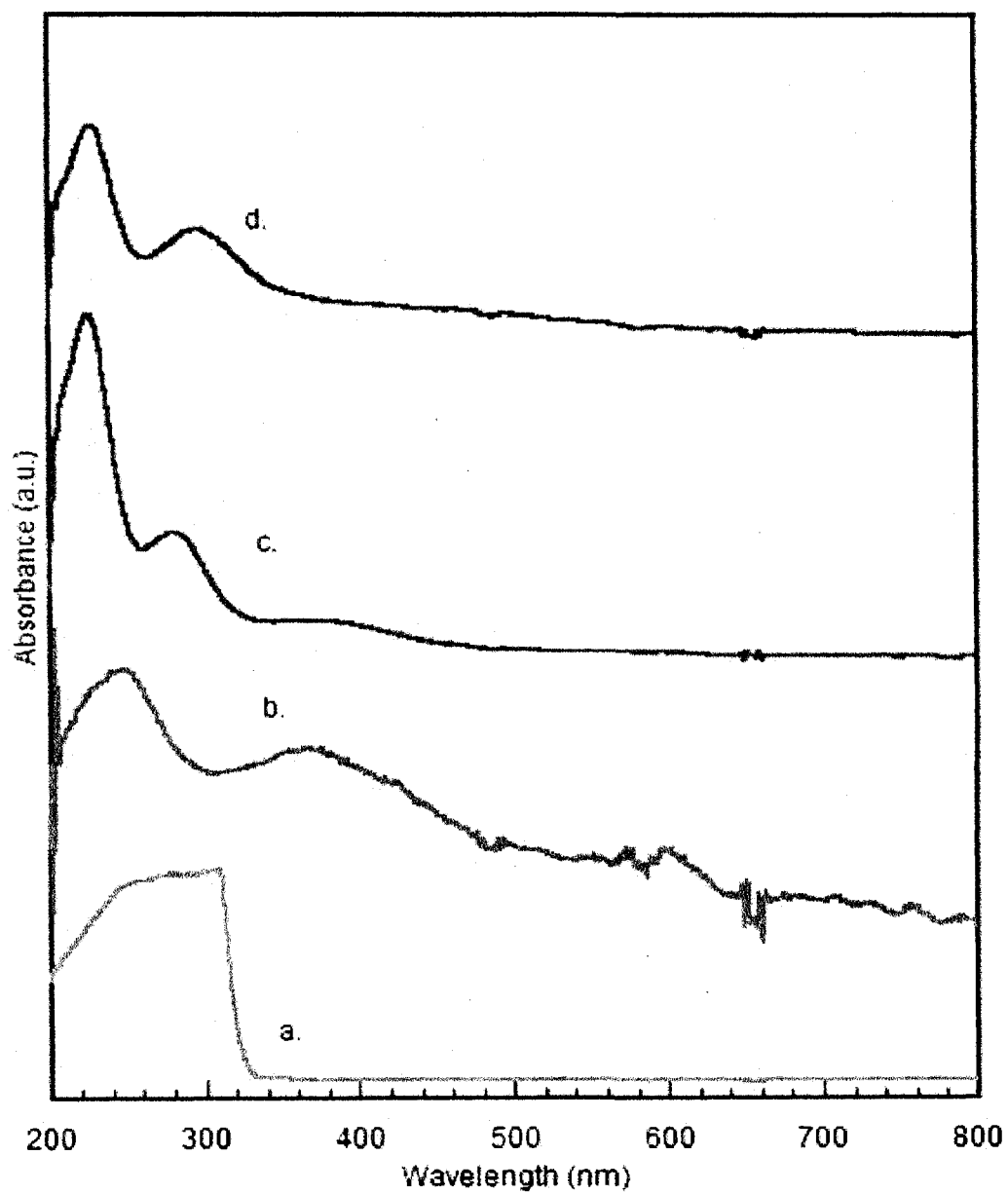


Figure 3.5: UV-Vis spectra of the materials from the reaction of K_2PdCl_6 with Aniline.

(a) Aniline (b) K_2PdCl_6 (c) Aniline/ PdCl_6^{2-} material with 1.0 M HClO_4 (d)

Aniline/ PdCl_6^{2-} material with 0 M HClO_4

3.3 Synthesis of N-phenyl-1,4-phenylenediamine/Palladium Materials

Literature reports have discussed the importance of oligomeric materials in the formation of PANI.²⁰⁻²² It has also been reported that oligomeric material may be just as conductive as PANI if enough units are present.²³ For example, the use of n-phenyl-1,4-phenylenediamine (NPPD) as the starting material in the synthesis of PANI has been achieved. In cases where the aniline monomer did not produce polymer, NPPD has been used to lower the potential barrier for oxidation and polymerization initiation. The question arises whether PANI formation using NPPD with a metal anion as the chemical oxidant will produce PANI/Pd composite materials. The method employed is identical to the synthesis using aniline. The palladium salts, PdCl_4^{2-} and PdCl_6^{2-} are used as the oxidant instead of ammonium persulfate in the synthesis. Figure 3.6 shows the schematic for the PANI/Pd synthesis using NPPD with PdCl_4^{2-} and PdCl_6^{2-} .

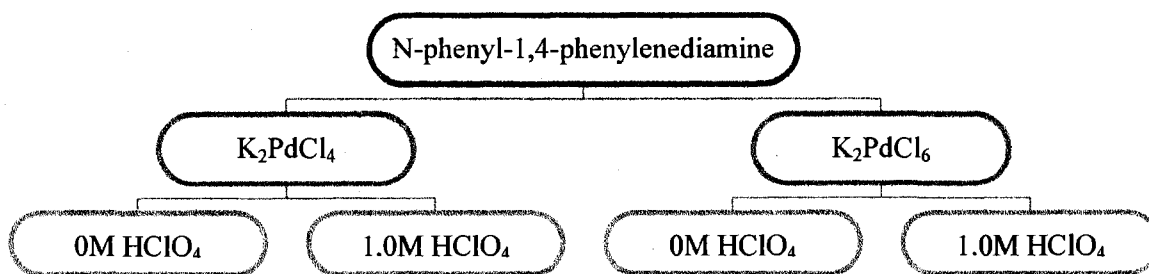


Figure 3.6: Schematic of the reaction of N-phenyl-1,4-phenylenediamine (NPPD) with palladium salts.

3.3.1 Synthesis of NPPD/Pd²⁺

The synthesis of PANI/Pd²⁺ materials was achieved by mixing 50 mL of 2.02 x 10⁻² M K₂PdCl₄ (Pd²⁺) with 50 mL of 0.11 M NPPD in the presence and absence of acid

(1 M HClO₄). The NPPD was added in excess to ensure complete reaction with the Pd anions. The final mole ratio of the aniline/metal was approximately 10:1. See Figure 3.6 for the schematic of the synthesis. The mixtures were left to react overnight. The product was vacuum filtered, washed with copious amount of water and stored in the desiccator.

The filtrates from all solutions were analyzed using the UV-Vis spectrometer (Figure 3.7). Each filtrate showed an excess of NPPD around 300 nm. The 1.0 M filtrate also had two broad peaks at 400 and 550 nm. It is difficult to determine where the 400 nm peak may be from due to the salt and NPPD both having broad bands in that region. The peak at 400 nm may be an artifact from the PdCl₄²⁻ or the formation of short chain oligomers.^{16-18,24,25}

The materials showed very similar absorption spectras as seen in Figure 3.5. Each has two distinct peaks at 210 and 290 nm. An important difference is the emergence of a broad peak at the 400 nm region, as stated previously, may be representative of the polaron- π^* transition in PANI. It is also possible that the peak observed at 290 nm is from the π - π^* transition from PANI. It is not conclusive, but the possibility of polymer formation may be favorable with NPPD as a starting material.

The 0 M HClO₄ material had an average yield of 1.0202 g \pm 0.0390 based on four subsequent trials. The 1.0 M HClO₄ material had an average yield of 0.5459 g \pm 0.0174 based on four synthetic trials. The materials had different colors indicating different compositions or different oxidation states.

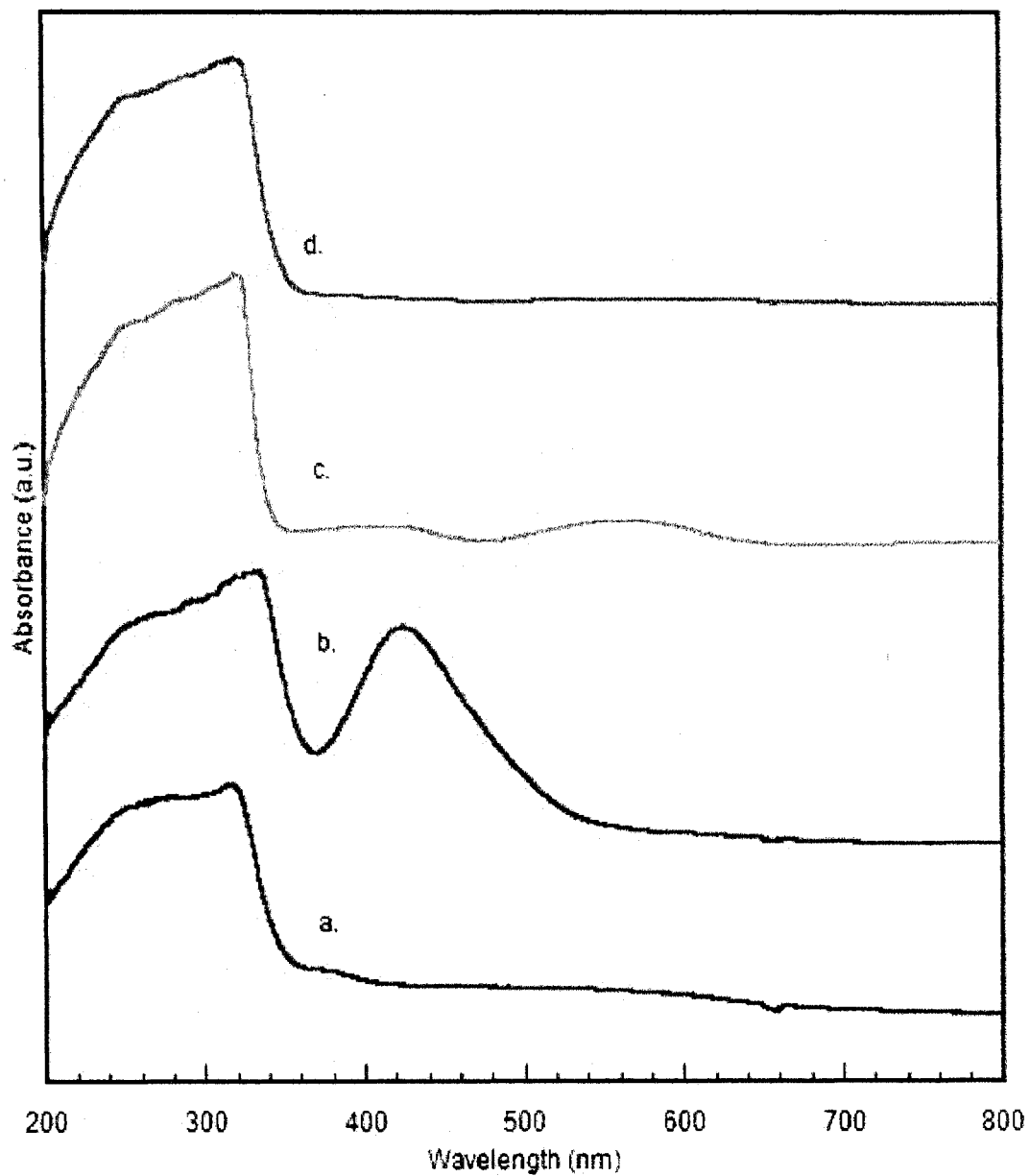


Figure 3.7 UV-Vis spectra of the filtrates from the reaction of K_2PdCl_4 with NPPD. (a) NPPD (b) K_2PdCl_4 (c) $\text{NPPD}/\text{PdCl}_4^{2-}$ material with 1.0 M HClO_4 (d) $\text{NPPD}/\text{PdCl}_4^{2-}$ material with 0 M HClO_4

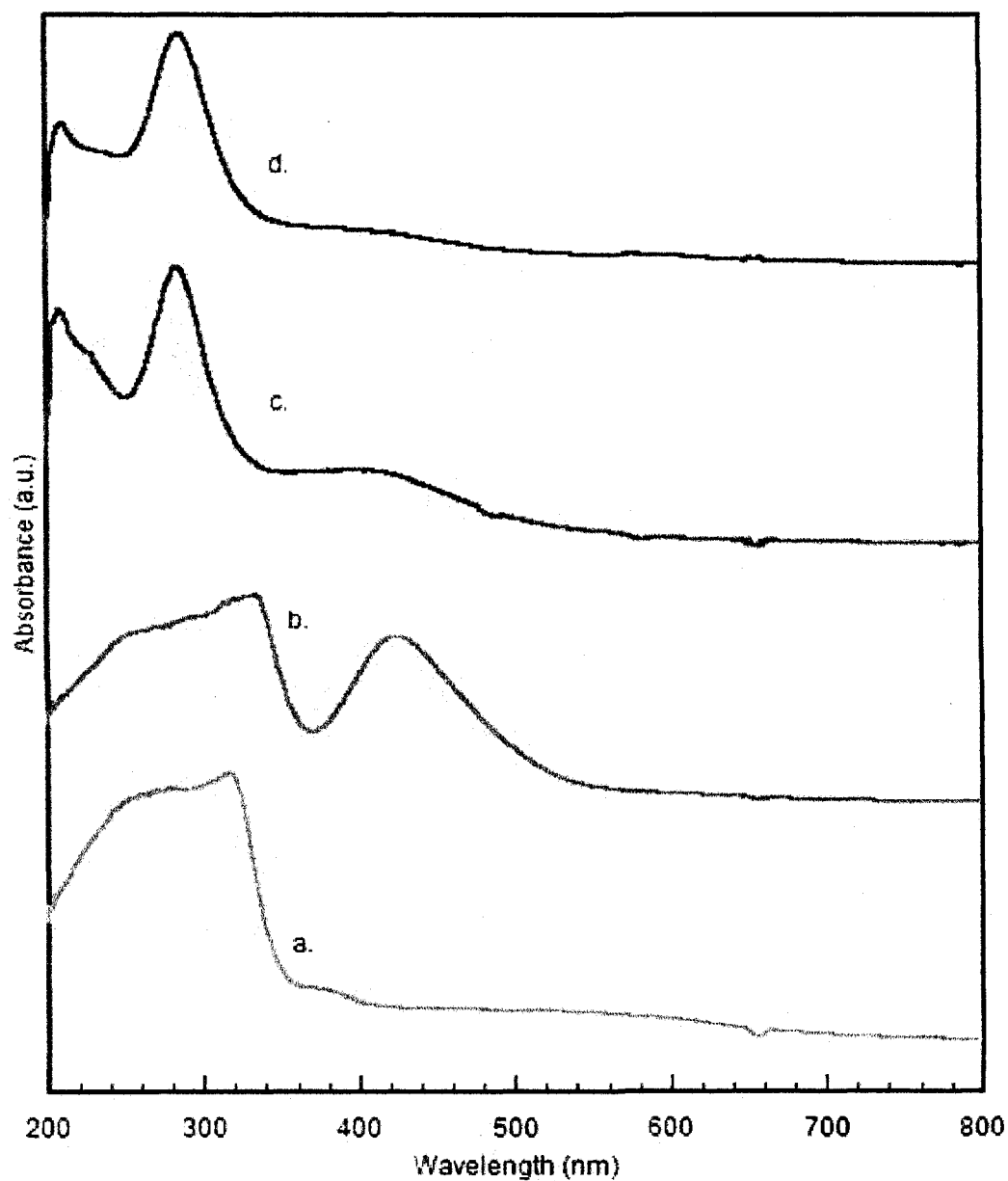


Figure 3.8 UV-Vis spectra of the materials produced from the reaction of K_2PdCl_4 with NPPD. (a) NPPD (b) K_2PdCl_4 (c) NPPD/ PdCl_4^{2-} material with 1.0 M HClO_4 (d) NPPD/ PdCl_4^{2-} material with 0 M HClO_4

3.3.2 Synthesis of NPPD/Pd⁴⁺

A similar synthetic route was used for the synthesis of NPPD/PdCl₆²⁻ materials. The synthesis of PANI/Pd⁴⁺ materials was achieved by mixing 50 mL of 1.20 x 10⁻² M K₂PdCl₆ (Pd⁴⁺) with 50 mL of 0.11 M NPPD in the presence and absence of acid (1 M HClO₄). The NPPD was added in a similar manner as aniline, in excess to ensure complete reaction. The final mole ratio of the aniline/metal was approximately 10:1. See Figure 3.6 for the schematic of the synthesis. The mixtures were left to react overnight. The product was vacuum filtered, washed with copious amount of water and stored in the desiccator.

The filtrates from all solutions were analyzed using the UV-Vis spectrometer (Figure 3.9). Each filtrate showed an excess of NPPD around 300 nm. The 1.0 M HClO₄ filtrate also had one broad peak at 400 nm, similar to its Pd²⁺ counterpart. It is difficult to determine where the 400 nm peak may be from due to the salt and NPPD both having broad bands in this region.

The materials, also analyzed on UV-Vis spectrometer, had very similar peaks even compared to the NPPD/Pd²⁺ complexes (Figure 3.10). The bands at 210 and 280 nm are characteristic to both 0 M HClO₄ and 1.0 M HClO₄. The 0 M HClO₄ material has a low, broad band at the 600 nm region, which may indicate that palladium was incorporated into the polymer. The 1.0 M HClO₄ spectra shows a broad peak at 420 nm, which again, may be representative of the polaron- π^* transition in PANI.

The 0 M HClO₄ material had a brown color and an average yield of 0.8051 g \pm 0.0441 for four synthetic trials. The 1 M HClO₄ material has a darker brown color

compared to the 0 M HClO_4 material and an average yield of $0.4820 \text{ g} \pm 0.0309$ for four synthetic trials.

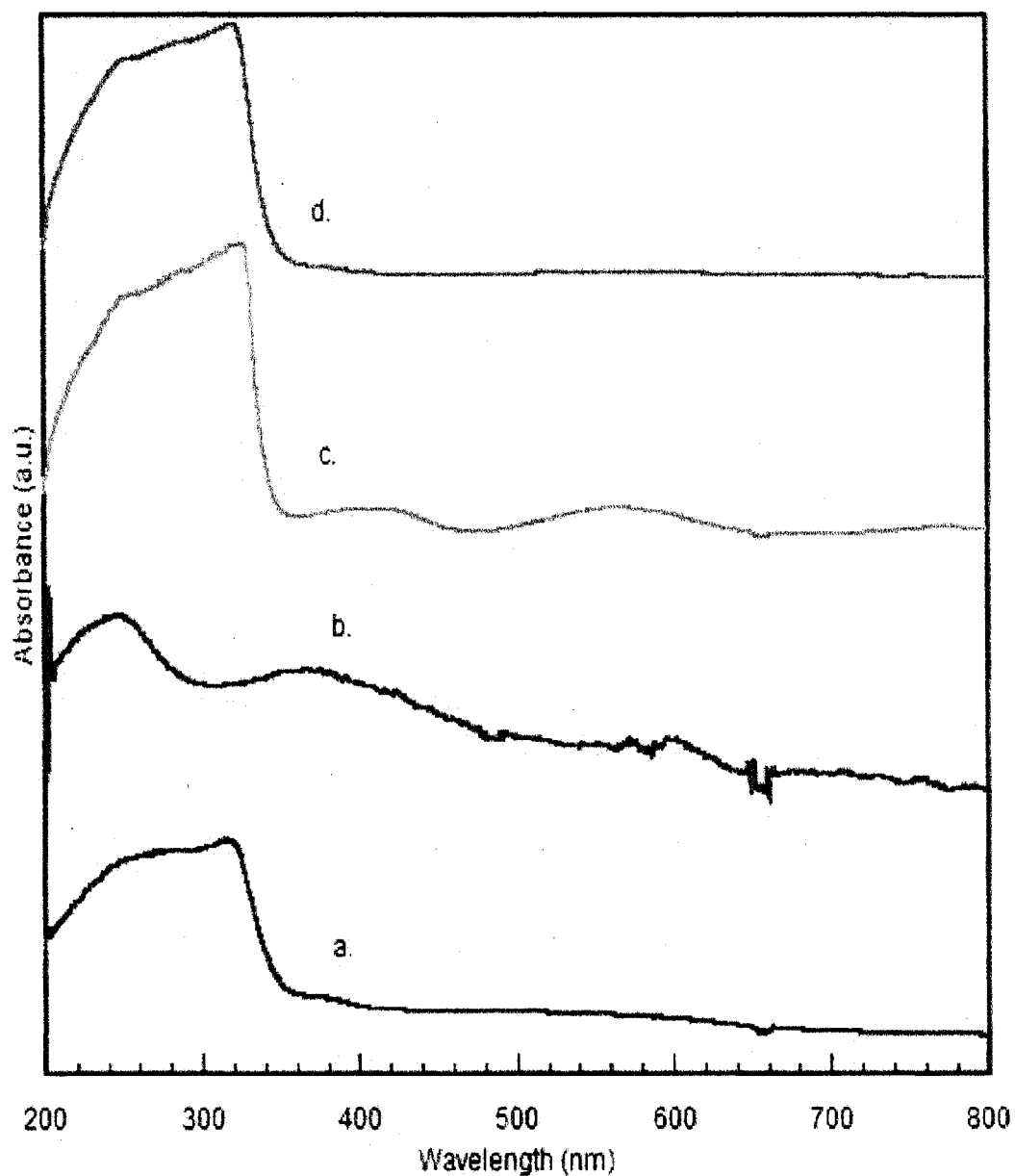


Figure 3.9: UV-Vis spectra of the filtrates from the reaction of K_2PdCl_6 with NPPD. (a) NPPD (b) K_2PdCl_6 (c) NPPD/ PdCl_6^{2-} material with 1.0 M HClO_4 (d) NPPD/ PdCl_6^{2-} material with 0 M HClO_4

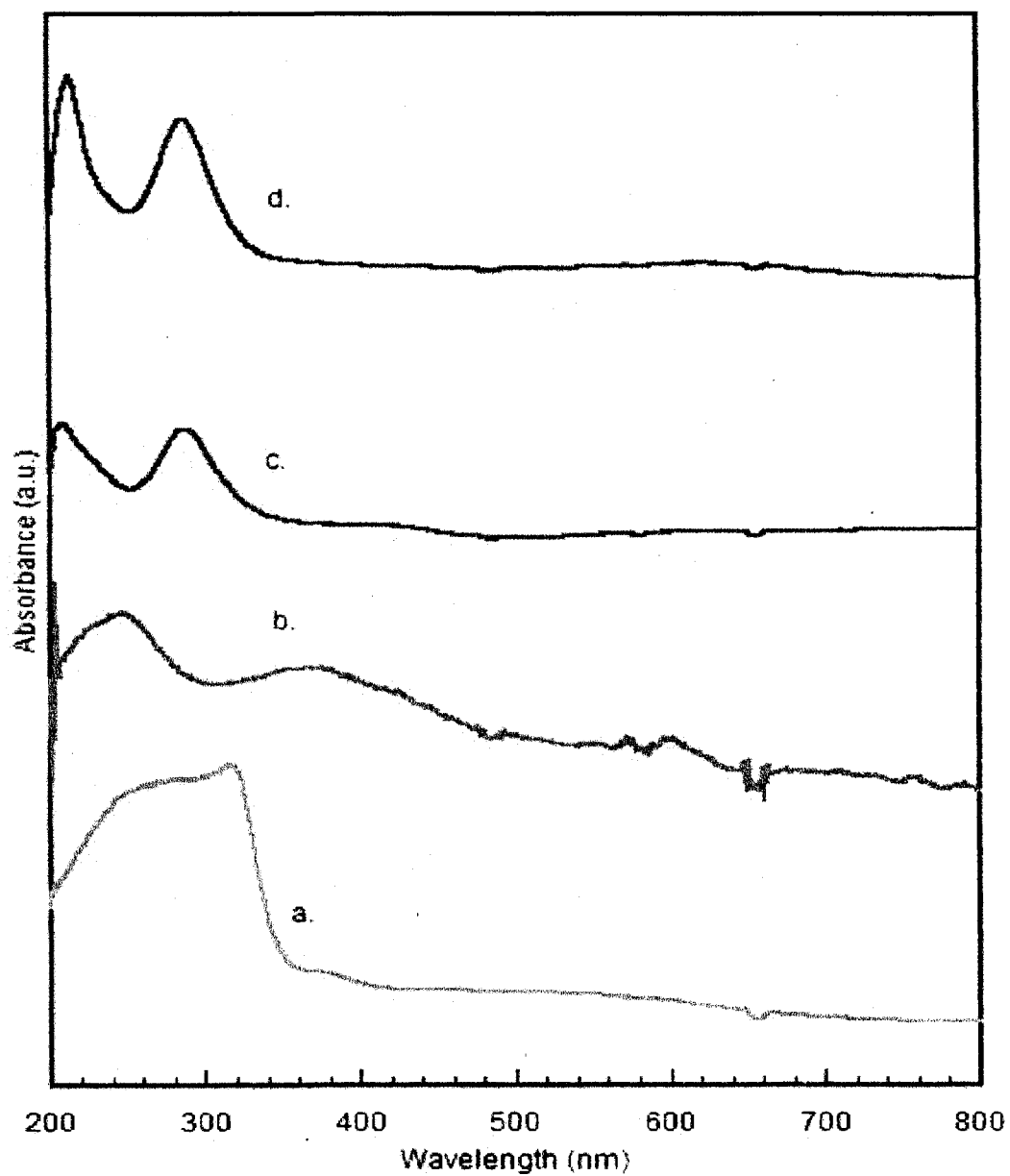


Figure 3.10: UV-Vis spectra of the materials produced from the reaction of K_2PdCl_6 with NPPD. (a) NPPD (b) K_2PdCl_6 (c) NPPD/ $PdCl_6^{2-}$ material with 1.0 M $HClO_4$ (d) NPPD/ $PdCl_6^{2-}$ material with 0 M $HClO_4$

3.4 Conclusion

From the preliminary UV-Vis spectroscopy data it is clear that the complete formation of PANI did not occur for any of our synthesis conditions. It is unclear yet, how much if any polymer exists in the materials. According to the UV-Vis spectra for the NPPD materials, there are characteristic bands that may be attributed to the formation of polymer. The intensities are very small suggesting that the polymer component in the material may be small.

Also, the absence of the band suggests that long chain polymer/metal composite is not the primary product. The lack of Pd in the filtrates suggests that the materials produced contain Pd. The filtrates show that very little, if any palladium salt was filtered through into the discarded solutions. The question remains whether the Pd is oxidized or reduced in the synthetic process.

3.5 References

- (1) Gospodinova, N.; Terlemezyan, L.; Mokreva, P.; Stejskal, J.; Kratochvil, P. *European Polymer Journal* **1993**, *29*, 1305-1309.
- (2) Armes, S. P.; Miller, J. F. *Synthetic Metals* **1988**, *22*, 385-393.
- (3) Stejskal, J.; Kratochvil, P.; Jenkins, A. D. *Polymer* **1996**, *37*, 367-369.
- (4) Patil, R. C.; Patil, S. F.; Mulla, I. S.; Vijayamohanan, K. *Polymer International* **2000**, *49*, 189-196.
- (5) Ray, A.; Asturias, G. E.; Kershner, D. L.; Richter, A. F.; MacDiarmid, A. G.; Epstein, A. J. *Synthetic Metals* **1989**, *29*, 141-150.
- (6) Stejskal, J.; Hlavata, D.; Holler, P.; Trchova, M.; Prokes, J.; Sapurina, I. *Polymer International* **2004**, *53*, 294-300.
- (7) Hasik, M.; Drelinkiewicz, A.; Wenda, E. *Synthetic Metals* **2001**, *119*, 335-336.
- (8) Drelinkiewicz, A.; Hasik, M.; Choczyński, M. *Materials Research Bulletin* **1998**, *33*, 739-762.
- (9) Syed, A. A. a. D., Maravattickal K. *Talanta* **1991**, *28*, 815-837.
- (10) Zhang, Z.; Wei, Z.; Wan, M. *Macromolecules* **2002**, *35*, 5937-5942.
- (11) Xu, Y.; Dai, L.; Chen, J.; Gal, J. Y.; Wu, H. *European Polymer Journal* **2007**, *43*, 2072-2079.
- (12) Wang, J.; Zhang, X.; Wang, Z. *Macromolecular Rapid Communications* **2007**, *28*, 84-87.
- (13) Chen, C.-H. *Journal of Applied Polymer Science* **2003**, *89*, 2142-2148.
- (14) Dan, A.; Sengupta, P. K. *Journal of Applied Polymer Science* **2007**, *106*, 2675-2682.

- (15) Kinyanjui, J. M.; Hatchett, D. W.; Smith, J. A.; Josowicz, M. *Chemistry of Materials* **2004**, *16*, 3390-3398.
- (16) Higuchi, M.; Imoda, D.; Hirao, T. *Macromolecules* **1996**, *29*, 8277-8279.
- (17) Neoh, K. G.; Young, T. T.; Looi, N. T.; Kang, E. T.; Tan, K. L. *Chemistry of Materials* **1997**, *9*, 2906-2912.
- (18) Venugopal, G.; Quan, X.; Johnson, G. E.; Houlihan, F. M.; Chin, E.; Nalamasu, O. *Chemistry of Materials* **1995**, *7*, 271-276.
- (19) Zhang, W. J.; Feng, J.; MacDiarmid, A. G.; Epstein, A. J. *Synthetic Metals* **1997**, *84*, 119-120.
- (20) Boyer, M. I.; Quillard, S.; Cochet, M.; Louarn, G.; Lefrant, S. *Electrochimica Acta* **1999**, *44*, 1981-1987.
- (21) Quillard, S.; Boyer, M. I.; Cochet, M.; Buisson, J. P.; Louarn, G.; Lefrant, S. *Synthetic Metals* **1999**, *101*, 768-771.
- (22) Wei, Y.; Yu, Y. H.; Zhang, W. J.; Wang, C.; Jia, X. R.; Jansen, S. A. *Chinese Journal of Polymer Science (English Edition)* **2002**, *20*, 105-118.
- (23) MacDiarmid, A. G.; Zhou, Y.; Feng, J. *Synthetic Metals* **1999**, *100*, 131-140.
- (24) Kinyanjui, J. M.; Wijeratne, N. R.; Hanks, J.; Hatchett, D. W. *Electrochimica Acta* **2006**, *51*, 2825-2835.
- (25) Genies, E. M.; Boyle, A.; Lapkowski, M.; Tsintavis, C. *Synthetic Metals* **1990**, *36*, 139-182.

CHAPTER 4

MATERIALS CHARACTERIZATION

4.1 Thermogravimetric Analysis

4.1.1 Introduction to Thermogravimetric Analysis

Thermal decomposition can give valuable information about the composition of a sample. The degradation will show distinct mass loss gradients that will correlate to the specific chemistry of a sample at a given temperature. In particular, the mass of palladium can be estimated through the thermal decomposition of organic material. Palladium has a melting point of 1554.9°C. PANI can have a melting point anywhere between 200°C when it is in the emeraldine base and 320°C when in the emeraldine salt state.¹⁻³ In addition, the organic component can be vaporized at high temperatures. Therefore, after a sample is heated up to 1250°C, the material remaining will primarily be palladium with some residual carbon content.

Some reports have found that degradation of the emeraldine base can begin as high as 400°C.³ Mass loss from around 110°C has been attributed to H₂O loss rather than polymer degradation.^{3,4} Figure 4.1 shows the thermal degradation of pure PANI. Initial mass loss occurs at 250°C, which indicates that the emeraldine state was synthesized. Further mass loss occurs from 300 to 600°C. This mass loss is indicative of structural degradation. It has been found that the mass change from 300 to 400°C may be attributed

to HClO_4 gas formed during the thermal process.⁴ A second explanation for the slight mass change from 300 to 400°C may be attributed to cross-linking of the polymer.^{3,5} Thermal treatment of PANI may result in cross-linking, which will render the material less volatile and requires a higher temperature to degrade.

Overall, a mass change of approximately 98% was observed for the chemically synthesized PANI. The crucible after each trial was empty, indicating that the polymer was completely decomposed and vaporized. There is some residual component of the polymer and dopant that remains in the crucible estimated at 2% of the total mass.

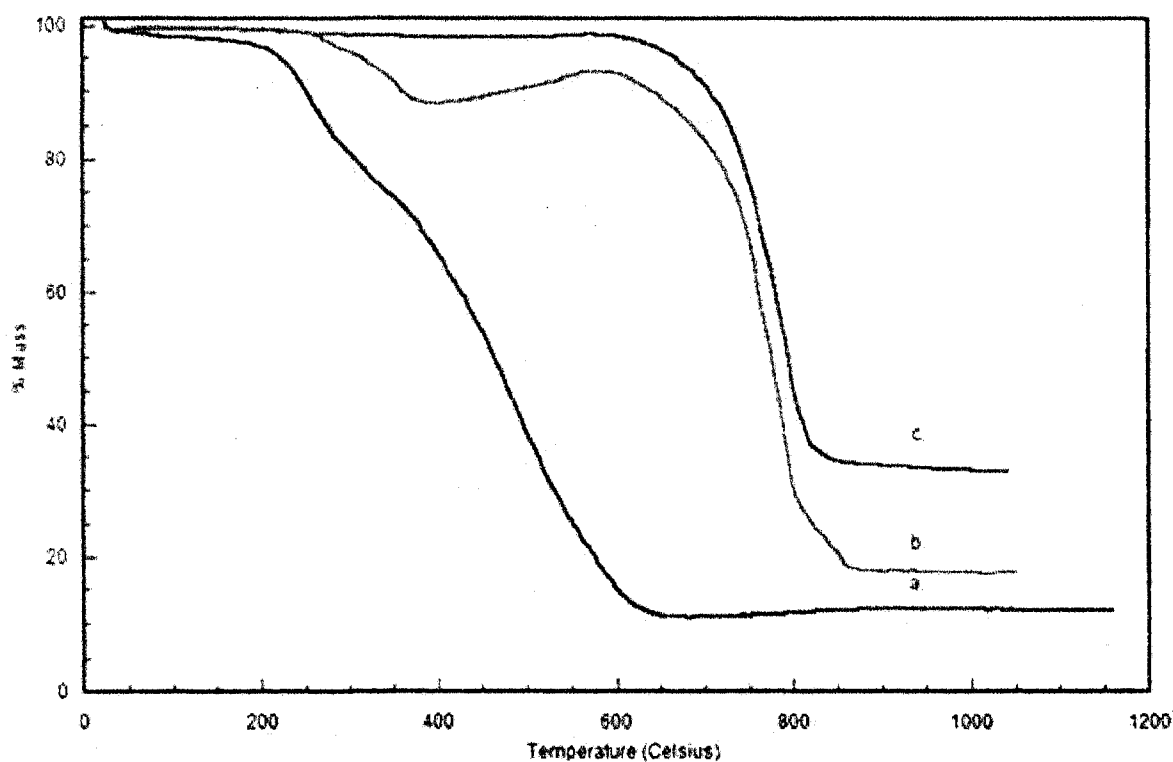


Figure 4.1 Thermogravimetric graph. a. chemically prepared PANI b. K_2PdCl_6 c. K_2PdCl_4

4.1.2 TGA of Aniline/Pd Composites

TGA on PANI/Pd composites has not been extensively studied previously. TGA was used as a preliminary method to estimate the total mass of palladium present in each solid. The differences between Aniline and NPPD solids can be compared in table 4.1. The percent mass loss for the aniline solids was averaged from 71-74%. This corresponds to a Pd composition of 26-29% for the materials produced using aniline. The thermal degradation signatures for the four materials prepared with aniline are shown in Figure 4.2. The materials produced from PdCl_4^{2-} have similar TGA signatures with a slight change observed for the materials produced with PdCl_6^{2-} and aniline. All materials show a sharp mass loss that begins around 280°C reaching a maximum loss at approximately 300°C. In addition, all materials show a smaller mass loss around 850°C. However, there are slight differences in the TGA for the materials produced with PdCl_4^{2-} and PdCl_6^{2-} . The materials produced with PdCl_6^{2-} have higher oxidative strength and can produce higher concentrations of the anilinium cations, which can produce higher molecular weight materials. The thermal decomposition of materials of higher molecular weight typically occurs at higher temperatures. It may also represent a higher degree of cross-linking in the materials. The data suggests that mixed materials may be obtained with PdCl_6^{2-} with more homogeneous materials obtained with PdCl_4^{2-} .

The final mass change at 850°C may be tied to the metal species and the residual organic components that cover the metal. As the organic component decomposes the metal can be coated with the chemical species. This coating is eventually desorbed as the temperature reaches 850°C. The fact that all four materials have this mass change at the same temperature implies that the process is tied to the thermally degraded organic

component and the remaining Pd metal. Another possible explanation for the mass change at 850°C may be attributed to the formation of oxides. The carrier gas in the TGA experiments is air, therefore the formation of PdO₂ may degrade at higher temperatures.

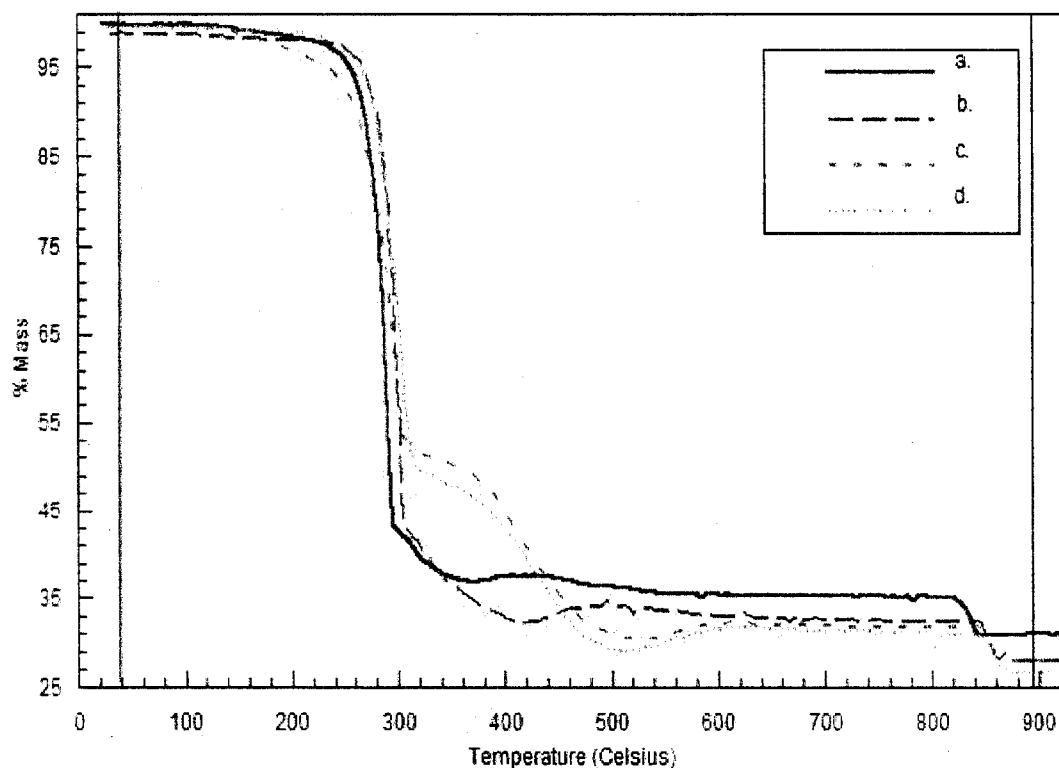


Figure 4.2 TGA of Aniline/Palladium materials a. 0M HClO₄ PdCl₄²⁻ b. 1.0M HClO₄ PdCl₄²⁻ c. 0M HClO₄ PdCl₆²⁻ d. 1.0M HClO₄ PdCl₆²⁻

4.1.3 TGA of NPPD/Pd Composites

There is no literature detailing the thermal degradation of NPPD/Pd materials. Therefore, comparison will be made using PANI prepared with aniline. The NPPD materials produced using PdCl₄²⁻ or PdCl₆²⁻ show a 79-92% mass loss. This corresponds to a Pd composition of 8-20%. Due to the lack of available aniline nitrogens for reaction, the decrease in Pd loading is expected relative to the organic component because the

species contains two aniline units in contrast to aniline. Figure 4.3 shows the TGA signature for the four materials produced using NPPD.

The thermal analyses of the materials produced using NPPD have similar signatures. The initial decomposition of all materials occurs at $\sim 200^{\circ}\text{C}$, which is approximately 80°C lower than the materials produced using aniline. A more noticeable change is also observed for the materials using NPPD with a much slower thermal decomposition between $300\text{--}620^{\circ}\text{C}$. This is consistent with the formation of higher molecular weight structures. This is enhanced with NPPD relative to aniline because the potential for oxidation is lowered as the number of aniline units increases. Therefore, the formation of higher molecular weight organic component is favorable. Finally, all materials show a small mass loss around 850°C consistent with materials produced using aniline with PdCl_4^{2-} and PdCl_6^{2-} .

All four of the materials, regardless of starting palladium salt, have similar thermal degradation characteristics. Initial degradation occurs at approximately 180°C , which can indicate the presence of short chain oligomers. The slope from 280 to 500°C may also be attributed to the formation of cross-linking from the thermal treatment in the crucible. Finally, at 860°C a drop in mass may also be attributed to bond breakage from cross-linking.

Unfortunately, TGA does not provide any information regarding the oxidation state of Pd in the materials. However, the thermal decomposition from heating the materials to 1250°C ultimately reduces any Pd^{2+} and Pd^{4+} to metallic Pd. The presence of metallic palladium can be observed in the crucible after the experiment is completed (Figure 4.4). Table 4.1 provides a summary of the Pd content and statistics associated

with the thermal analysis of the materials produced using aniline, NPPD, PdCl_4^{2-} or PdCl_6^{2-} .

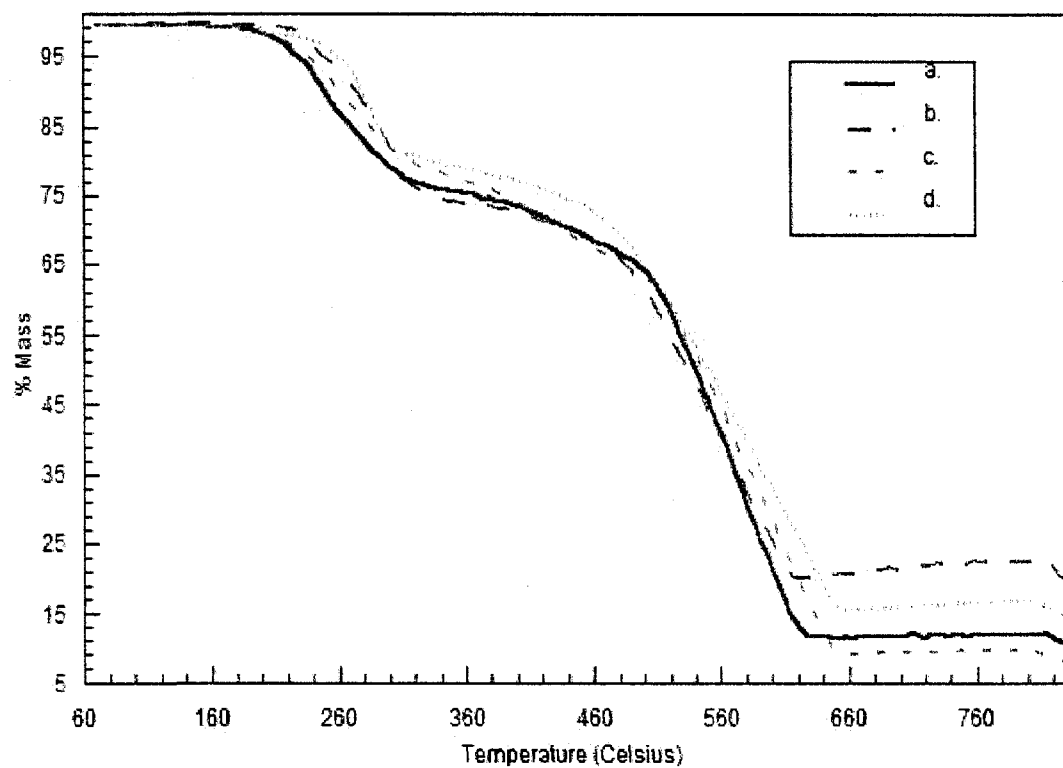


Figure 4.3 TGA of NPPD/Palladium materials a. 0M HClO_4 PdCl_4^{2-} b. 1.0M HClO_4 PdCl_4^{2-} c. 0M HClO_4 PdCl_6^{2-} d. 1.0M HClO_4 PdCl_6^{2-}

Aniline				
	0M HClO ₄ Pd ²⁺	1 M HClO ₄ Pd ²⁺	0M HClO ₄ Pd ⁴⁺	1 M HClO ₄ Pd ⁴⁺
% Organic composition	72.82	73.94	72.97	71.03
% rsd	3.33	1.64	0.73	0.07
% Pd composition	24.76	24.85	26.50	28.92
Range	27.29	26.09	27.04	28.97

NPPD				
	0M HClO ₄ Pd ²⁺	1 M HClO ₄ Pd ²⁺	0M HClO ₄ Pd ⁴⁺	1 M HClO ₄ Pd ⁴⁺
% Organic composition	90.33	79.44	91.38	88.35
% rsd	1.96	0.00	0.66	0.94
%Pd composition	7.90	20.56	8.02	10.82
Range	9.71	20.56	8.62	11.66

Table 4.1 Average % mass loss and standard deviations of 3 separate trial runs.

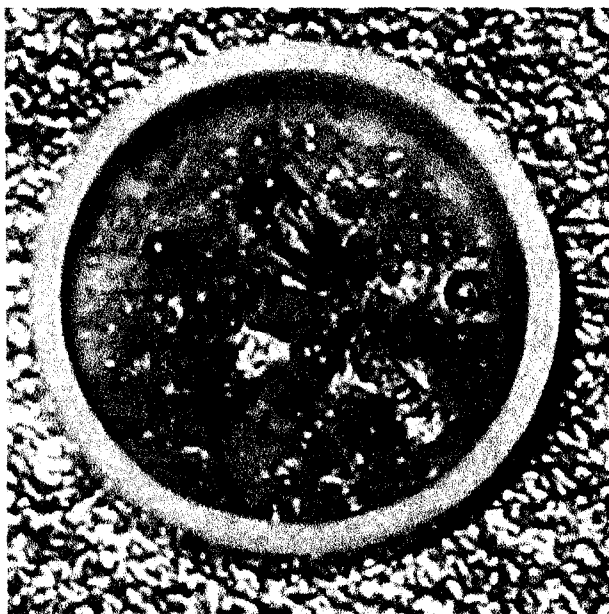


Figure 4.4 Image of crucible after thermal analysis.

4.2 Scanning Electron Microscopy

4.2.1 Introduction to Scanning Electron Microscopy

SEM imaging provided information regarding the physical morphology of each material. Figure 4.5 shows the SEM image of pure PANI. The material shows random orientations and geometries of the amorphous solid with open porosity. The introduction of the palladium species in PANI should influence the morphology of the sample. The SEM studies presented will examine the influence of the two different organic units (aniline, NPPD) on the morphology of the materials produced using both PdCl_4^{2-} and PdCl_6^{2-} as chemical oxidants. In addition, the use of acid in the synthesis will be explored to determine if polymer formation is inhibited as suggested by the published mechanism.⁶ Therefore, SEM will be used to provide visual information regarding the morphological differences of materials formed using the reaction scheme defined previously.

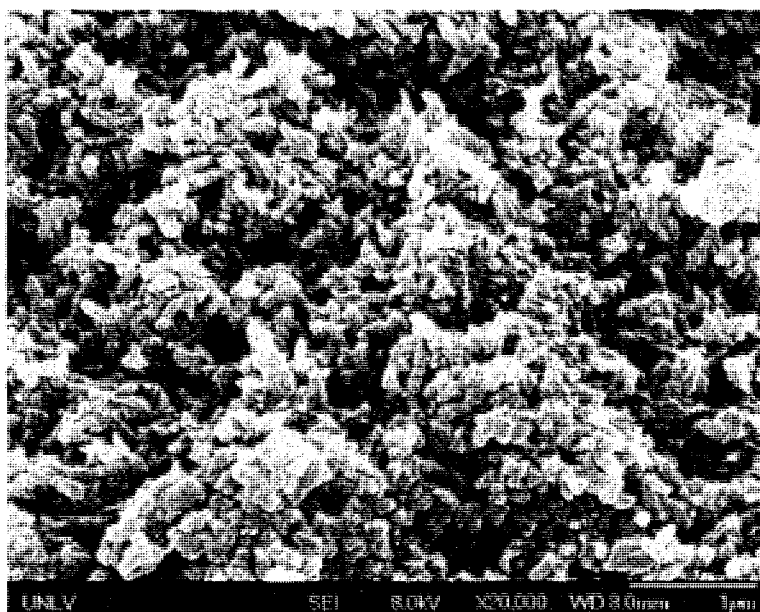


Figure 4.5 SEM image of pure chemically synthesized PANI

4.2.2 Aniline and Palladium Complexes

SEM images of the materials produced using the aniline monomer are shown in Figure 4.6 and Figure 4.7. The samples were gold coated to remove charging effects. The high charge interference is due to the insulating properties of the materials. All of the samples produced using either PdCl_4^{2-} or PdCl_6^{2-} with aniline required Au films consistent with the formation of complex materials rather than conductive polymer. It can be concluded that the synthesis using PdCl_4^{2-} and PdCl_6^{2-} as the chemical oxidant does not produce highly conductive polymer.

The SEM image of the material produced using 0 M HClO_4 PdCl_4^{2-} and aniline supports the formation of the Pd/aniline complex. The material exhibits flat, sheet-like structures that look to be crystalline in nature. The material produced shows uniform dimensions on the order of 100-150 nm in width and 1000-2000 nm in length for the composite. A direct comparison with pure PANI shows that the material has a much different morphology indicative of the formation of a different material.

A more drastic change is seen with the addition of acid (1.0 M HClO_4) for the aniline/ PdCl_4^{2+} . Flat planar sheets are observed with much larger overall dimensions. In contrast to the material produced using no acid, the dimension of the complex materials are much larger, on the order of 10 microns for some of the species in the SEM. Lower magnification was used to show the overall magnitude difference in the structures. This complex may again have crystalline properties based on the planar molecular geometry observed for all material in the image. Neither of the materials morphology compares favorably with PANI. In addition, previous studies of PANI with other metal salts such as PdCl_6^{2-} have produced materials that show bulk metal as spheres and the polymer.^{7,8}

There are no spherical Pd deposits in these images suggesting that the Pd species may not be fully reduced.

Interestingly, the 0 M HClO_4 PdCl_6^{2-} solid has characteristics of both amorphous and crystalline materials. There are the rod-like formations as well as flat sheets. The 1.0 M HClO_4 PdCl_6^{2-} solid has the flat, smooth planar sheets that are similar to the 1.0 M HClO_4 PdCl_4^{2-} solid. Without acid, the structures appear to contain amorphous as well as crystalline morphologies. PdCl_6^{2-} is a stronger oxidant, which may give rise to the formation of more oligomeric materials in the final product. However, when acid is utilized, the material appears as flat planar sheets, although for all samples present there are no visible metal particles. The lack of visible metal particles does not indicate a lack of palladium. TG analysis shows that palladium is approximately 20-30% by mass. It may be an indication that the palladium particles are too small to be detected in the range it was imaged. Another possibility is that the palladium may be located in the bulk of the material as opposed to the surface.

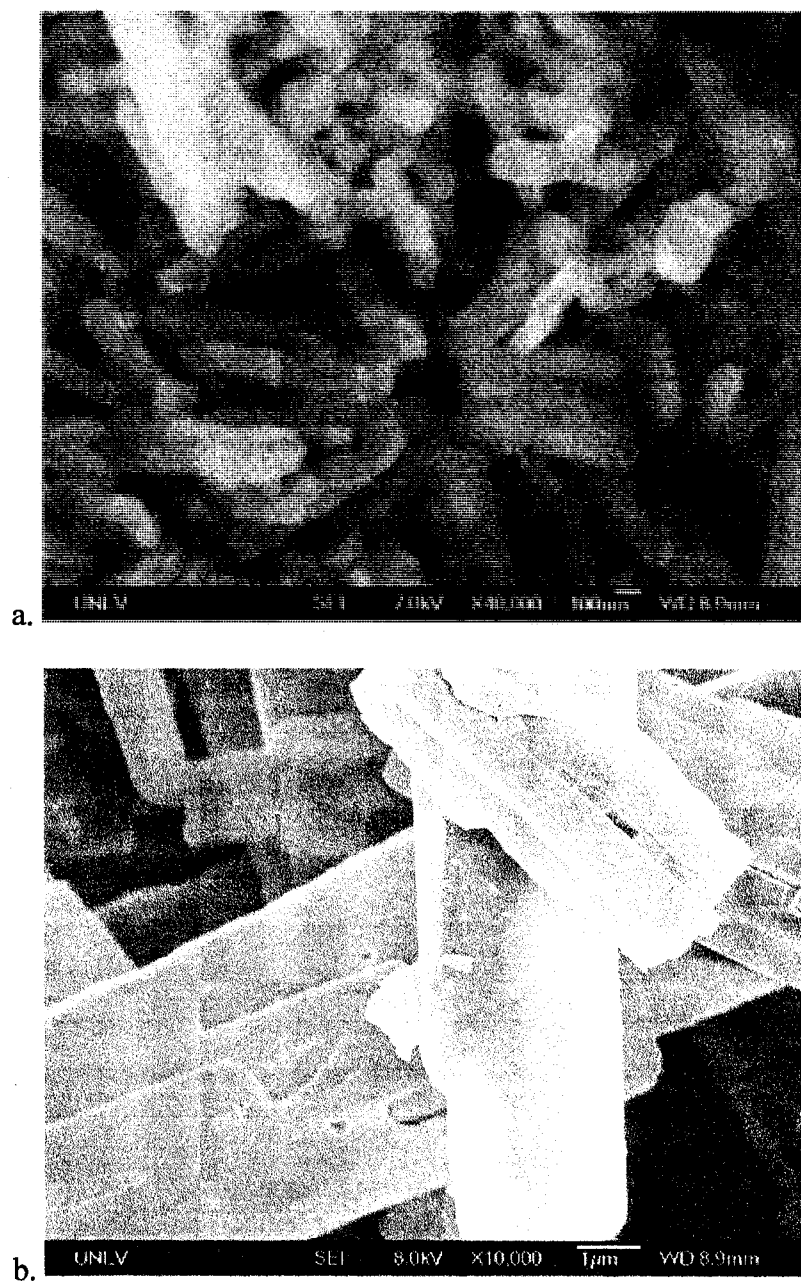


Figure 4.6 SEM images of Aniline and Palladium complexes a. Aniline/ PdCl_4^{2-} in 0M HClO_4 b. Aniline/ PdCl_4^{2-} in 1.0M HClO_4

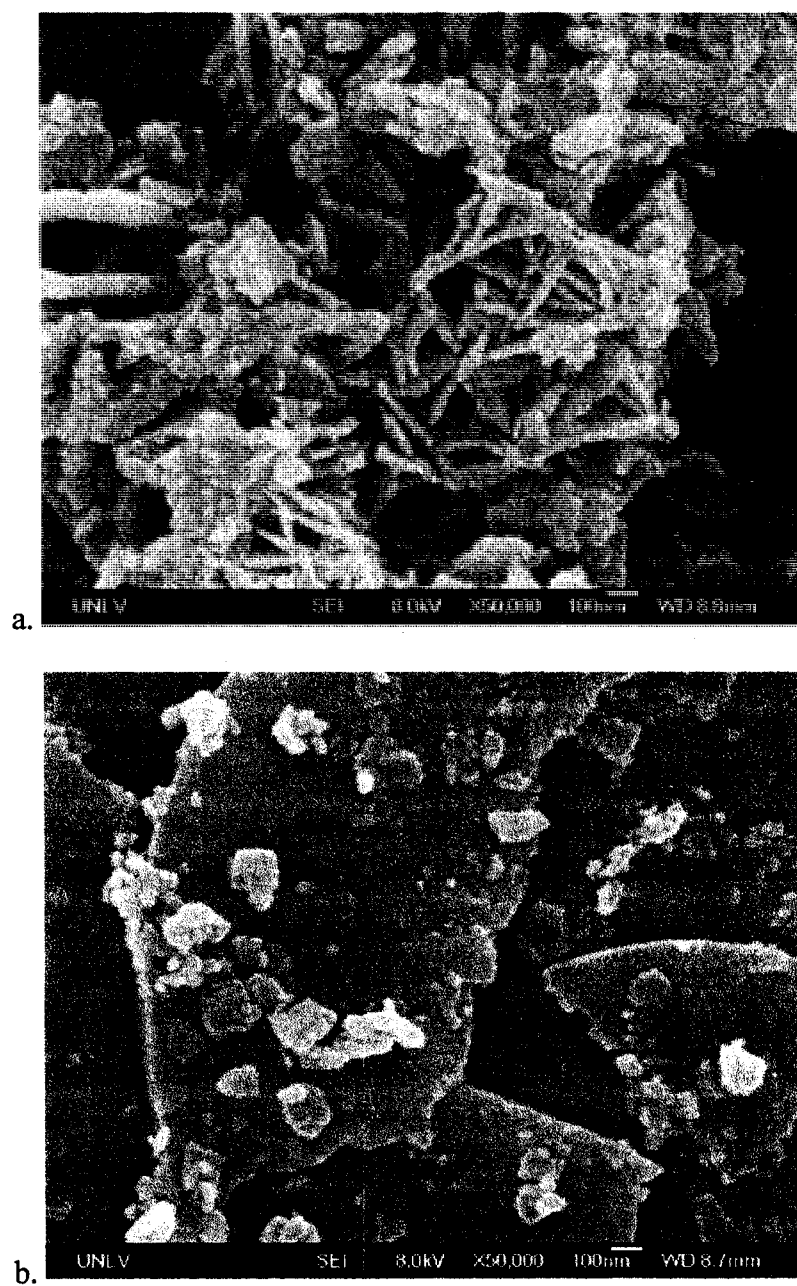


Figure 4.7 SEM images of Aniline and Palladium complexes a. Aniline/ PdCl_6^{2-} in 0M HClO_4 b. Aniline/ PdCl_6^{2-} in 1.0M HClO_4

4.2.3 NPPD and Palladium Composites

It has been previously shown that PANI can be produced from NPPD using ammonium persulfate as the chemical oxidant.⁷ Therefore, NPPD was reacted with either PdCl_4^{2-} or PdCl_6^{2-} in solutions with and without 1 M HClO_4 to enhance the formation of polymer rather than the complexes observed for aniline. Figure 4.8 and Figure 4.9 shows images from the four NPPD composites. The low composition of Pd in the samples suggests either higher molecular weight material is formed or that Pd is not incorporated readily into the materials.

The SEM images of the materials produced using NPPD with the Pd^{2+} show a more amorphous morphology when compared to the materials produced using aniline. All of the materials show very similar morphology without any flat, planar sheets. It is apparent that longer chain length materials are formed regardless of acid content. However, a certain amount of layering is still observed for the NPPD samples with PdCl_4^{2-} used to produce the materials. This layering is diminished for samples produced using PdCl_6^{2-} . The results suggest that the materials may be a mixture of composite material with more amorphous, oligomeric material.

These materials require gold coating to minimize charge effects prior to imaging consistent with low conductivity. This suggests that the oligomeric component is not sufficiently high to improve the conductivity of the materials. It also supports the possibility that NPPD/Pd complex formation might occur contributing to the low conductivity. Regardless, these materials do not possess the conductive properties of pure PANI-EB consistent with all materials produced using aniline.

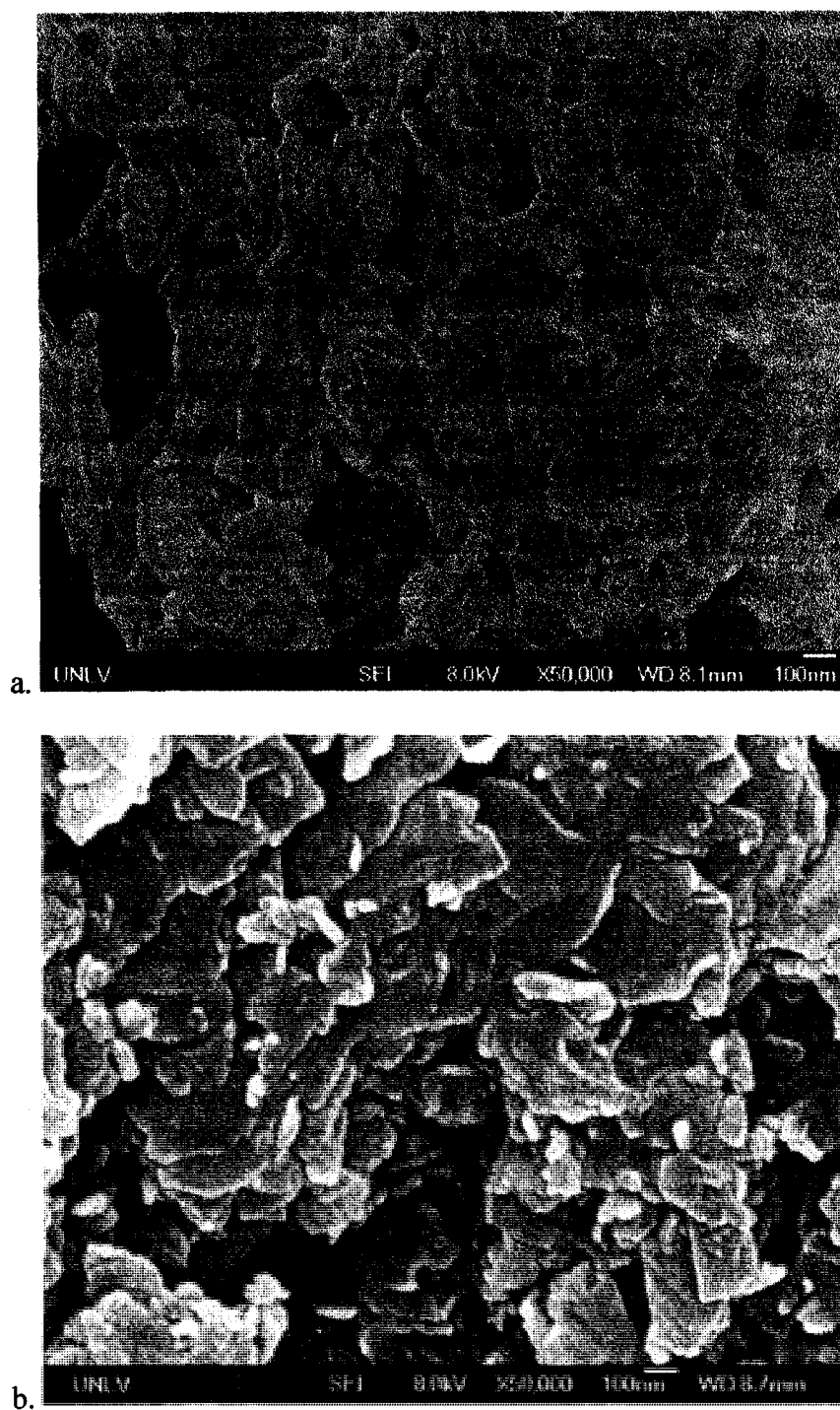


Figure 4.8 SEM images of n-phenyl-1,4-phenylenediamine and Palladium composites a. NPPD/ PdCl_4^{2-} in 0M HClO_4 b. NPPD/ PdCl_4^{2-} in 1.0M HClO_4

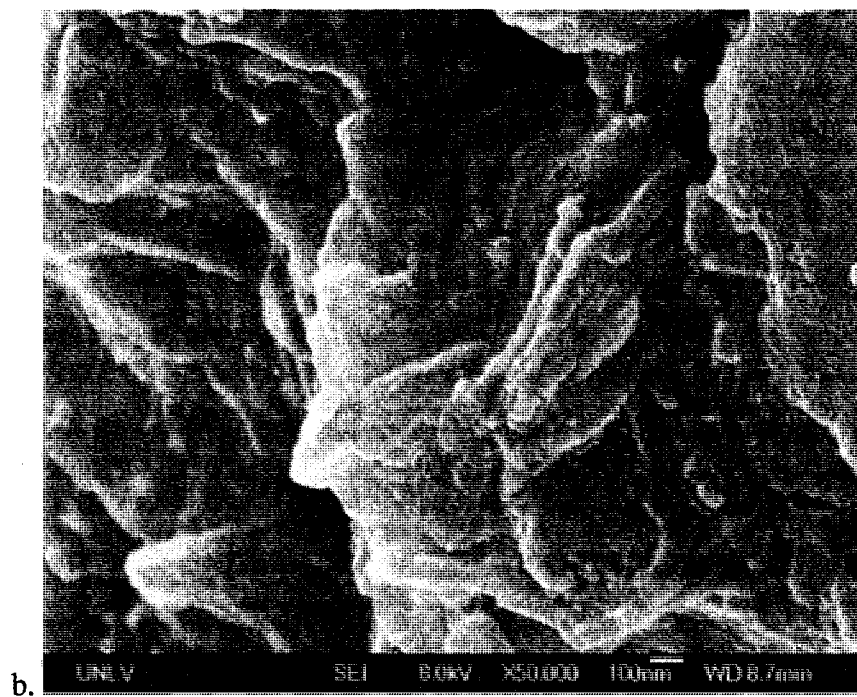
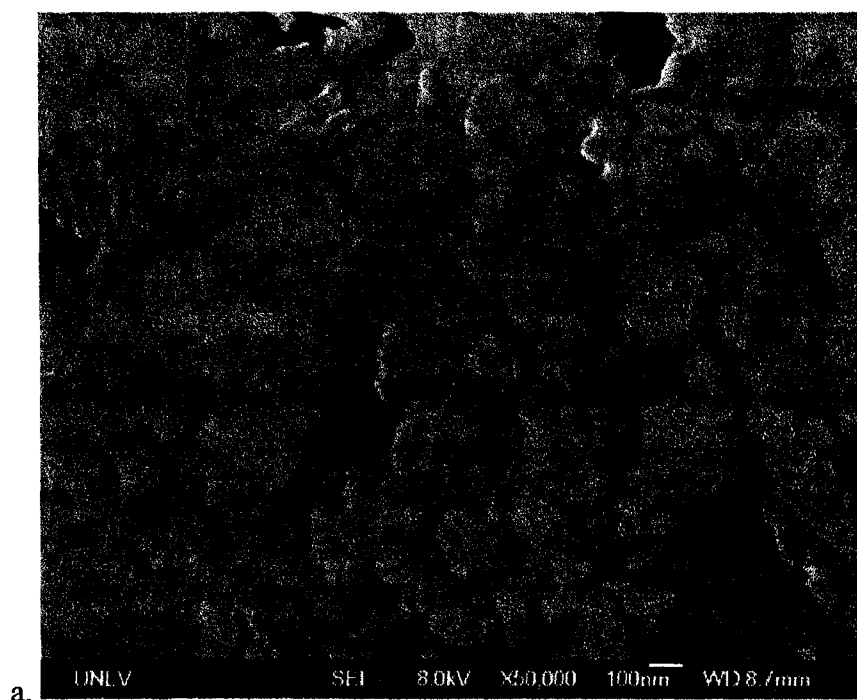


Figure 4.9 SEM images of n-phenyl-1,4-phenylenediamine and Palladium composites a. NPPD/ PdCl_6^{2-} in 0M HClO_4 b. NPPD/ PdCl_6^{2-} in 1.0M HClO_4

4.3 Fourier-Transform Infrared Spectroscopy

4.3.1 Introduction to Fourier-Transform Infrared Spectroscopy

FTIR spectroscopy is used to probe the chemistry of all materials produced. Information regarding the polymeric nature and the chemical structure can be obtained using FTIR spectroscopy. In particular, PANI has characteristic peaks that are associated with the polymer, which can be monitored in the materials produced in these studies. For example the C-N-C peak at 1295 cm^{-1} is indicative of long polymer chain formation and can be monitored to determine if polymer is produced.⁹ The intensity of that band when compared to that of pure PANI alone will strongly indicate the degree of polymerization that exists for each material.

In addition, the bands associated with the benzenoid and quinoid aromatic structures can be examined to determine the extent of oxidized species incorporated into each material. The benzenoid structure band is observed at 1490 cm^{-1} with two bands for the more oxidized quinoid structure observed at 1570 cm^{-1} and 1086 cm^{-1} . Additional bands in the fingerprint region at 821 cm^{-1} are indicative of the out-of-plane C-H bond for the aromatic structures.⁹ A ratio of the benzenoid to quinoid structures for PANI is one when it is in the emeraldine base form. The ratio represents a 50/50 distribution of these structures. Figure 4.10 shows the PANI spectra with the corresponding structures.

4.3.2 FTIR of Aniline and Palladium Complexes

The FTIR analysis of the materials produced using aniline and PdCl_4^{2-} and PdCl_6^{2-} is presented in Figure 4.11. Analysis of the region associated with the formation at PANI at 1295 cm^{-1} shows very little IR absorbance for any of the materials produced using aniline and PdCl_4^{2-} regardless of the acid concentration. There is a small component of

polymer material that emerges when PdCl_6^{2-} is used as the chemical oxidant. For all material produced the FTIR spectra support the predominant formation of the Pd/Aniline complexes rather than polymeric materials. Similar complexes have been observed previously when functionalized aniline was reacted with Pd^{2+} . However, it is obvious that the pure PANI and the aniline complexes are not the same.¹⁰⁻¹²

The emergence of low intensity C-N bands, indicative of polymer formation can be observed in the FTIR spectra for the aniline/ PdCl_6^{2-} materials. This is consistent with the formation of oligomeric materials due to the relatively higher oxidative strength PdCl_6^{2-} in comparison to PdCl_4^{2-} . It can be concluded that polymer is present in the bulk of the materials produced in these studies. However, the overall FTIR signature is consistent with the formation of Aniline/Pd complexes rather than polymer.

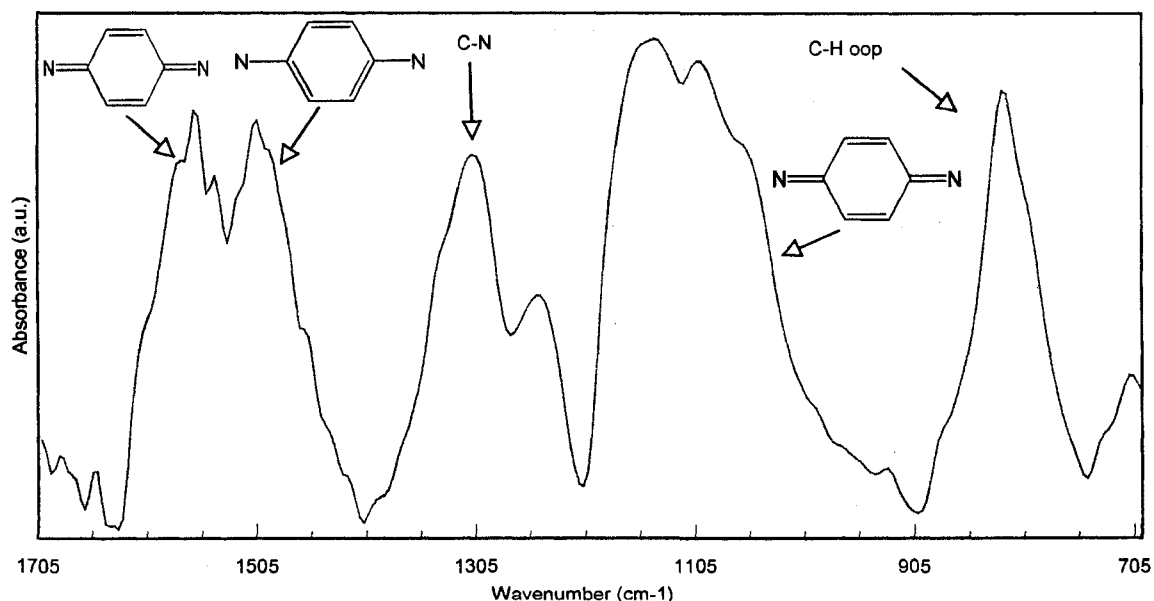


Figure 4.10 FTIR of pure PANI

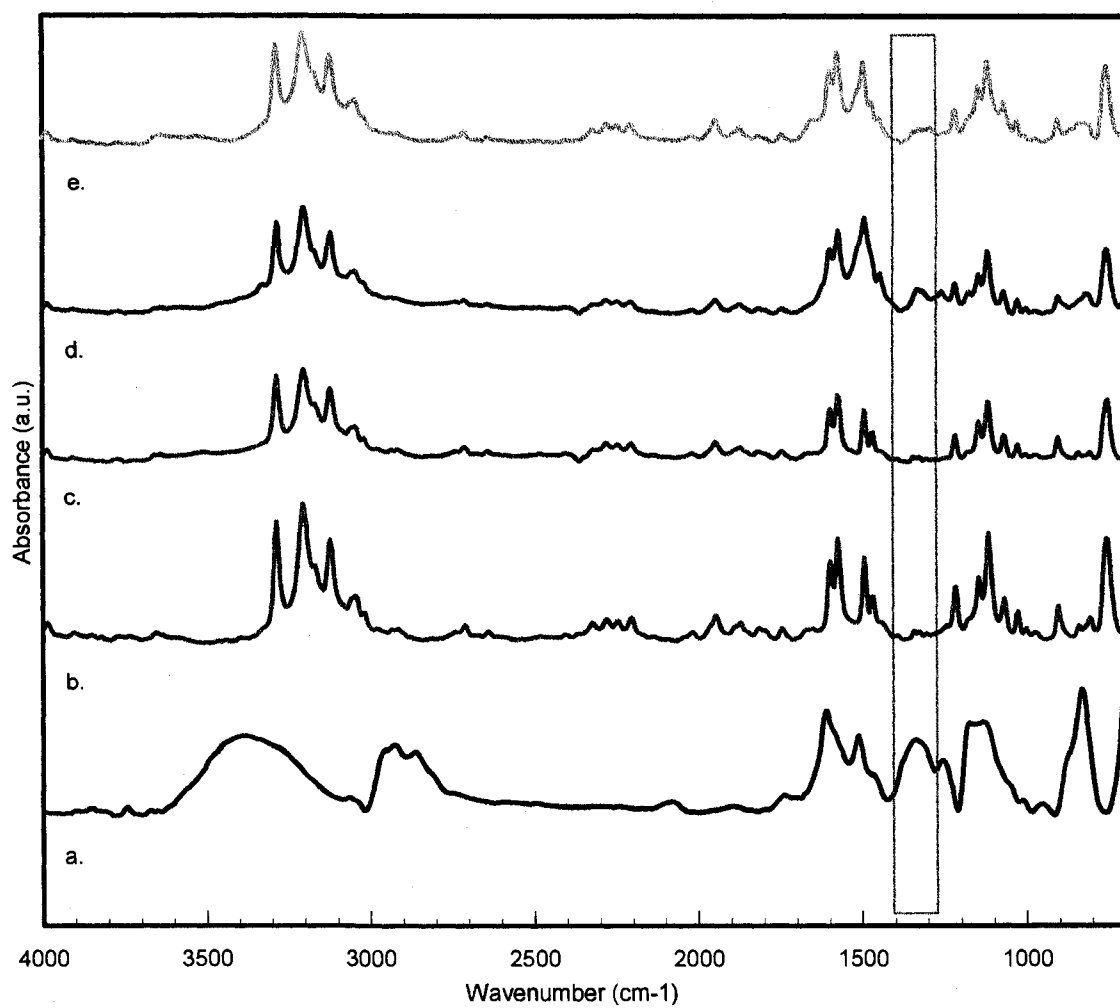


Figure 4.11 FTIR of Aniline and Palladium complexes a. pure PANI b. 0M HClO_4 PdCl_4^{2-} c. 1.0M HClO_4 PdCl_4^{2-} d. 0M HClO_4 PdCl_6^{2-} e. 1.0M HClO_4 PdCl_6^{2-}

4.3.3 FTIR of NPPD and Palladium Complexes

The use of NPPD as a starting material in the synthesis using PdCl_4^{2-} and PdCl_6^{2-} provides a secondary material that is more polymeric in nature in comparison to aniline. It is expected based on the SEM image in section 4.2 that the materials will be more polymeric in comparison to materials produced using aniline. The FTIR spectra for materials produced using NPPD are presented in Figure 4.12.

The signature of polymeric material can be observed at 1295 cm^{-1} for every material produced using NPPD regardless of the chemical oxidant or acid concentration. The FTIR spectra of these materials compare favorably to pure PANI. The imaging data suggested that these materials were more polymeric in nature than the aniline materials. NPPD favors polymer formation because the starting material is dimeric and can be more readily oxidized than aniline due to the relatively higher electron density. Bands associated with the benzenoid and quinoid peaks for 1.0 M HClO_4 PdCl_4^{2-} and 1.0 M HClO_4 PdCl_6^{2-} are similar to PANI with less line splitting and broadening of the bands consistent to polymer formation. The C-N band at 1295 cm^{-1} is visible in each solid, which is indicative of polymer formation. Another noteworthy observation is that some of the weaker IR overtone bands have disappeared. For instance, the bands from 1700 to 2400 cm^{-1} indicate the aromatic nitrile functional group (C-N), are not present in any of the FTIR for PdCl_6^{2-} .

Interestingly, the 1.0 M HClO_4 PdCl_6^{2-} most closely matches pure PANI. This material also has low palladium loading at 12%. The low Pd loading in this sample may be attributed to a lack of fully reduced Pd due to the formation of complexes. These materials can be incorporated into the polymer as defect structures providing relatively

low Pd loading for this material. However, with the exception of one material (Pd^{2+} , NPPD, 1 M HClO_4) the Pd loading is significantly diminished when compared to the materials produced using aniline indicating that polymer formation does not necessarily improve the percent of Pd incorporated into the final material.

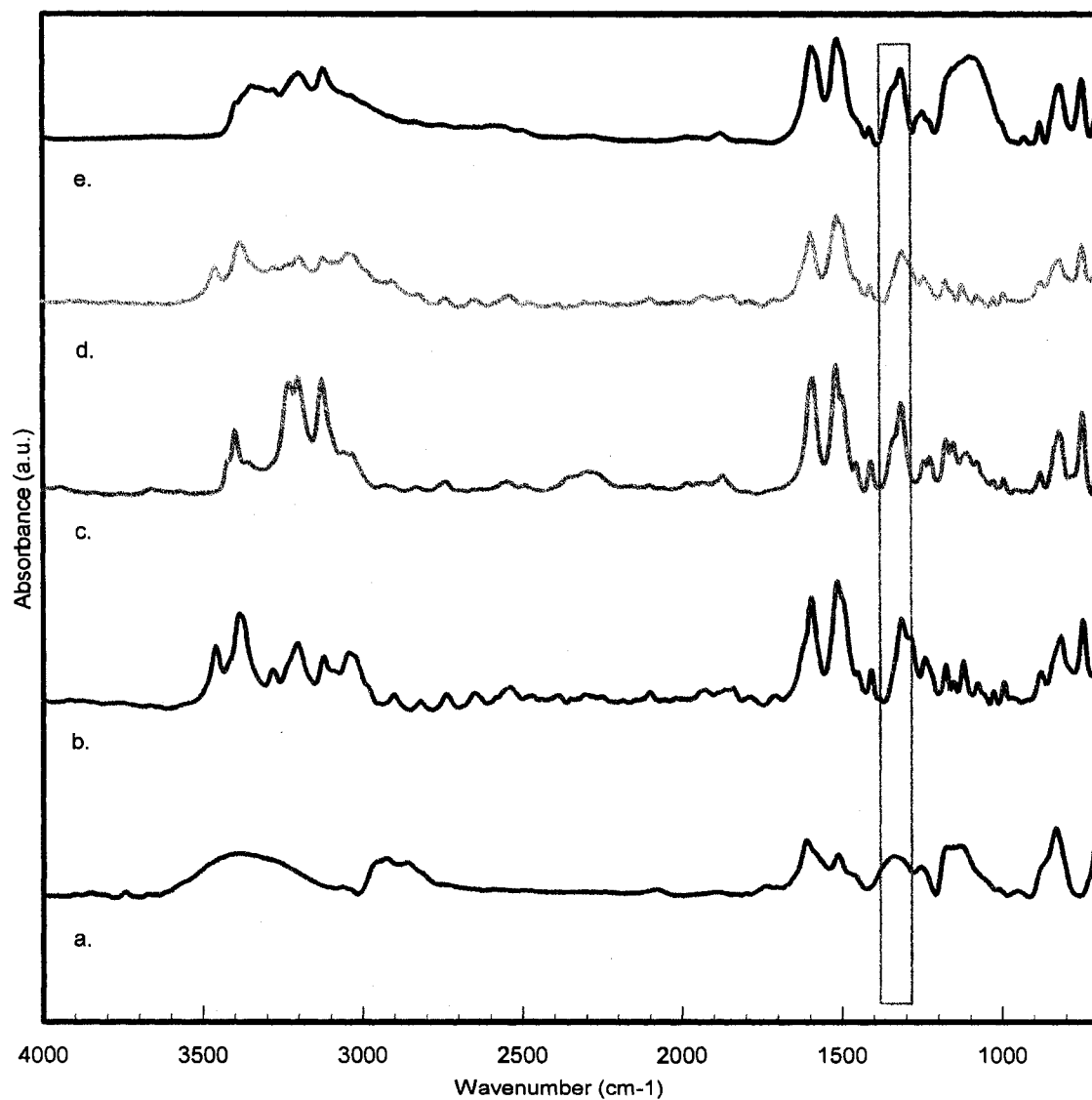


Figure 4.12 FTIR of NPPD and Palladium composites a. pure PANI b. 0M HClO_4 PdCl_4^{2-} c. 1.0M HClO_4 PdCl_4^{2-} d. 0M HClO_4 PdCl_6^{2-} e. 1.0M HClO_4 PdCl_6^{2-}

4.4 X-ray Photoelectron Spectroscopy

4.4.1 Introduction to X-ray Photoelectron Spectroscopy

XPS is a useful tool in determining the surface chemical characteristics of solid state materials. PANI is simplistic in nature because only three elements will theoretically be present in the XPS spectra. Nitrogen, Carbon, and Hydrogen will be the largest contributors of mass, whereas the acid doping of PANI may be present in diminished quantity. In this case, HClO_4 may show some chloride and oxygen bands. In our studies the application of this technique will be focused on elucidation of the oxidation state of palladium as incorporated into the materials prior to thermal or chemical treatment. This data is will only focus on the aniline/Pd complexes.

4.4.2 XPS of Aniline with PdCl_4^{2-} and PdCl_6^{2-}

The XPS survey for aniline reacted with PdCl_4^{2-} and PdCl_6^{2-} with and without acid is shown in Figure 4.13. The XPS data shows bands consistent with N, O, Cl, C, and Pd. The appearance of Cl and O can be attributed to either the reduction of the oxidants (K_2PdCl_4 or K_2PdCl_6) or the acid (HClO_4). Similar to SEM measurements, the samples were found to be insulating. The effect of low conductivity can be seen as an induced shift to higher binding energies. Since it was determined previously that these solids do not contain polymeric material, the characteristic PANI peaks of C-C, C-H and $\text{C}=\text{C}^{13}$ are absent. This is conclusive evidence that the aniline prepared materials are not polymeric.

The presence of palladium is observed in the XPS survey for both samples (Figure 4.14). This confirms the TGA data suggesting that the materials contain significant amounts of Pd. However, the oxidation state of the Pd species is unknown. To analyze these samples without the effect of charge interference, the technique of X-

ray Excited Auger Electron Spectroscopy (XAES) was used also to determine the oxidation state of palladium. For comparison Pd foil was examined providing binding energies of 335.2 eV and 327.6 eV for XPS and XAES, respectively. The spectra in Figure 4.12 show a distinct shift to higher binding energies for all materials produced using aniline with PdCl_4^{2-} and PdCl_6^{2-} for the Pd 3d bands. The energy difference was approximately 10 eV higher than metallic Pd. Thus, the species is oxidized relative to the Pd foil which is consistent with either the formation of a complex or the oxidation of reduced Pd in the sample to PdO. It is impossible to know if the signal is due to one or the other or a combination of the both materials. However, the data clearly shows that the Pd is not metallic. Also, the values for the salts and PdO and PdO₂ are listed on the graph and show that the materials are not purely in those states either.

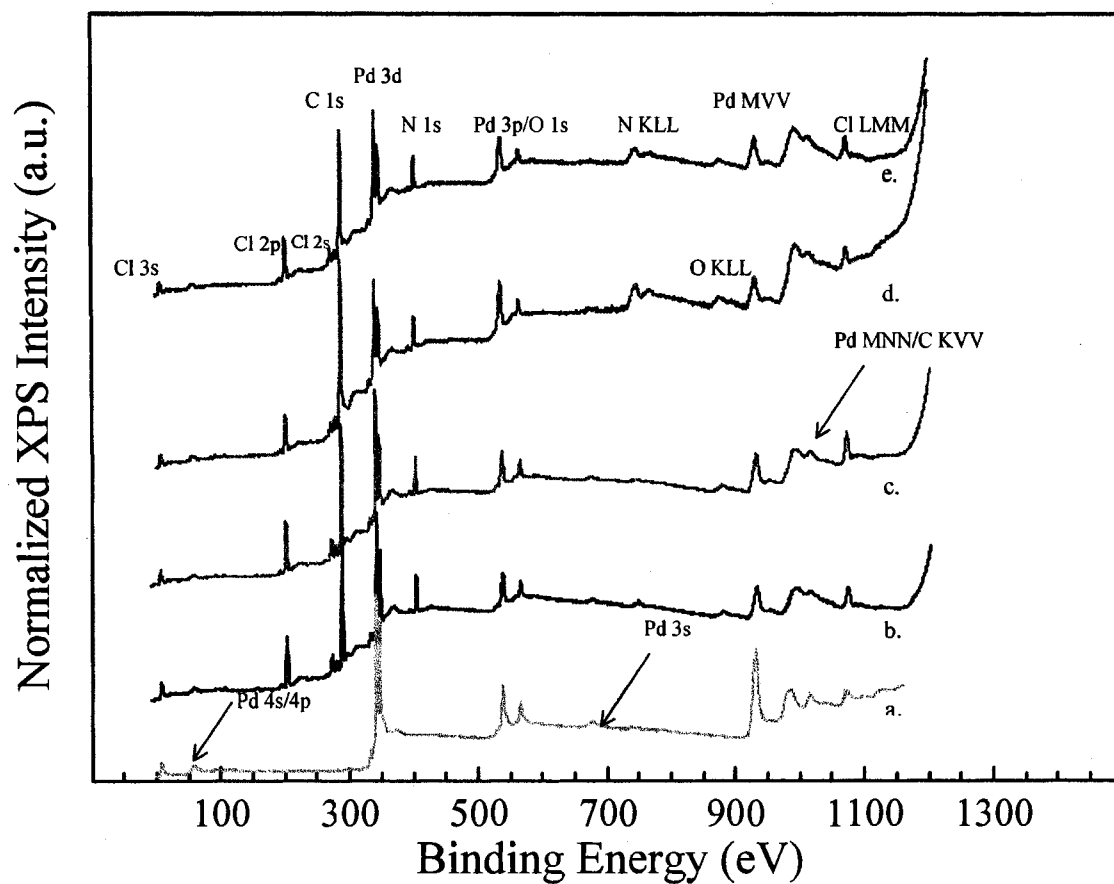


Figure 4.13 XPS survey of a. Palladium foil b. 0M HClO₄ PdCl₄²⁻ in Aniline c. 1.0M HClO₄ PdCl₄²⁻ in Aniline d. 0M HClO₄ PdCl₆²⁻ in Aniline e. 1.0M HClO₄ PdCl₆²⁻ in Aniline. Data prepared by Sujitra Pookpanratana.

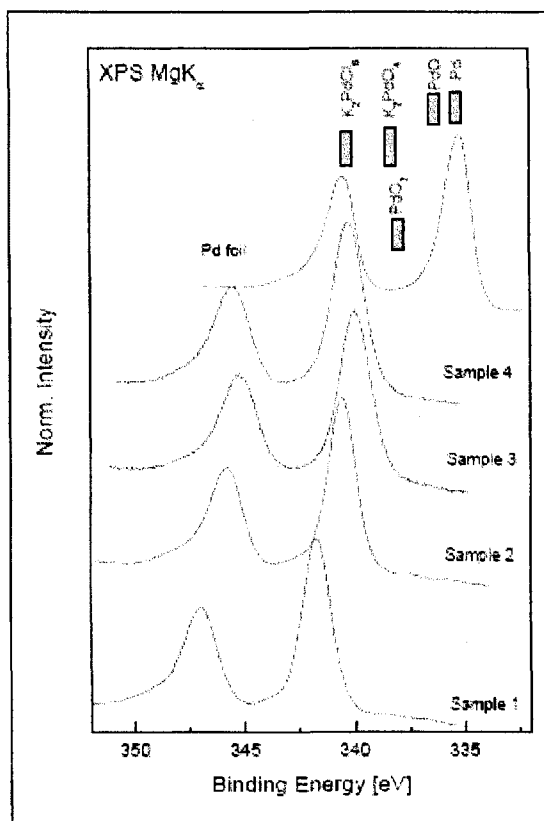


Figure 4.14 XPS of Pd 3d bands of Pd foil, 0M HClO₄ PdCl₄²⁺ in Aniline (Sample 1), 1.0M HClO₄ PdCl₄²⁺ in Aniline (Sample 2), 0M HClO₄ PdCl₆²⁺ in Aniline (Sample 3), 1.0M HClO₄ PdCl₆²⁺ in Aniline (Sample 4). Image and data prepared by Sujitra Pookpanratana

4.5 Sodium Borohydride Reduction

Chemical methods can be employed to reduce the Pd complex to form Pd⁰.

Therefore, samples were further treated with reducing agent sodium borohydride, NaBH₄ to convert the materials. The influence of NaBH₄ on the organic components of the material is unknown. It is assumed that any organic component will also be reduced.

The question remains whether the material will be converted to polymer in the process of reducing Pd. The polymer or organic component can also be reduced in the process.

For the reactions approximately 30 mg of each material was ground to uniform consistency and mixed with 10 mL of water. All samples were be sonicated for approximately fifteen minutes to ensure dispersion of the material in the water. A 1 mL aliquot of 0.13 M NaBH₄ (0.05 g/10 mL) was added to the materials. The solutions were allowed to react for 24 hours and the resulting materials were collected by filtration and washed copiously with water to remove any residual soluble solution species.

4.5.1 FTIR of NaBH₄ and PANI

As stated previously, FTIR analysis of the materials provides an indication of the polymeric composition. The influence of NaBH₄ on the formation of polymer in the process of reducing the Pd species is of general concern. Figure 4.15 compares pure PANI with NaBH₄ reacted PANI. In the pure PANI spectra, the peaks at 1490 cm⁻¹ and 1500 cm⁻¹ are showing that the benzenoid and quinoid units are not equal. After addition of NaBH₄, The composition changes with a benzenoid peak and a smaller quinoid peak. Correspondingly, the band at 1080 cm⁻¹ is reduced in intensity, corresponding to the quinoid structure. The FTIR data indicates that the treated polymer is more reduced than the EB form of PANI. All characteristic peaks for PANI are present after NaBH₄ reduction, which indicates that the integrity of the polymer is maintained.

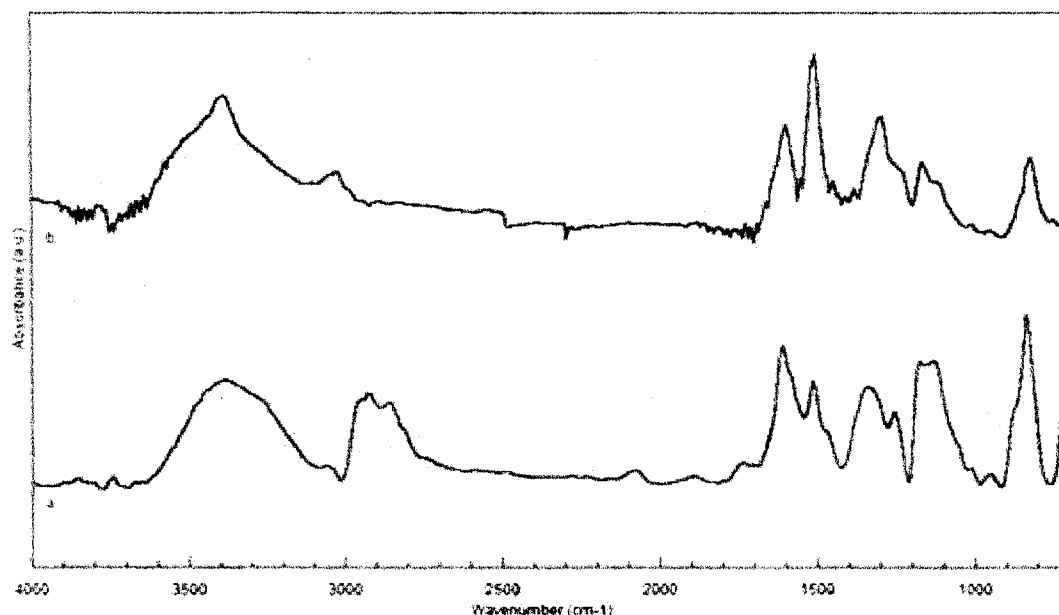


Figure 4.15 FTIR spectra of (a) pure chemically prepared PANI and (b) PANI reacted with NaBH_4

4.5.2 SEM of NaBH_4 Reduced Solids

SEM analysis of the materials produced after reaction with NaBH_4 for the products obtained from preliminary reactions with material produced using 0M HClO_4 PdCl_4^{2-} , 1.0M HClO_4 PdCl_4^{2-} , 0M HClO_4 PdCl_6^{2-} , and 1.0M HClO_4 PdCl_6^{2-} with aniline have been carried out. The SEM images are shown in Figure 4.16 and Figure 4.17.

For the material produced using PdCl_4^{2-} , aniline and 0 M HClO_4 we observed small flat, planar sheets of material with uniform dimension and defined morphology (Figure 4.16). The material is much different when treated with NaBH_4 showing larger chunks of material with variable morphology. Upon closer inspection, small sphere-like structures also appear at the edge of the material. For the partially reacted material produced with PdCl_4^{2-} and aniline in 1.0 M HClO_4 small spheres of material are visible. The material aggregates as it accumulates on the surface with granular morphology. It is

impossible to determine from the images if Pd metal exists and is encapsulated during the reaction. However, the reduction process clearly changes the composition of the materials. Similarly, the material produced using PdCl_6^{2-} with aniline in 0 M HClO_4 shown a material that is predominantly granular in morphology (Figure 4.17). As suggested previously, these materials may contain a small amount of polymer with a higher amount of Pd complex. Therefore, the reduction of Pd may free the organic component to react and form polymeric structures that were not previously possible.

In contrast, the material produced using PdCl_6^{2-} with aniline in 1 M HClO_4 did not change appreciably. At this point we are unsure why the material did not react with NaBH_4 to produce materials comparable to the first three examples. One possibility is that Pd in the material is not efficiently reduced due to the chemical differences that exist in the material. It may require that longer reaction times be employed to fully convert the material. However, further experiments are required to determine if this is the case.

All samples examined using SEM after reaction with NaBH_4 required gold coatings to be imaged due to charging effects. This implies that the reduction did not produce highly conductive polymer. However, the reaction was not carried out in acid and therefore acid doping of any polymer that formed does not occur. Acid doping in PANI is critical in enhancing the conductivity of the material.^{9,14}

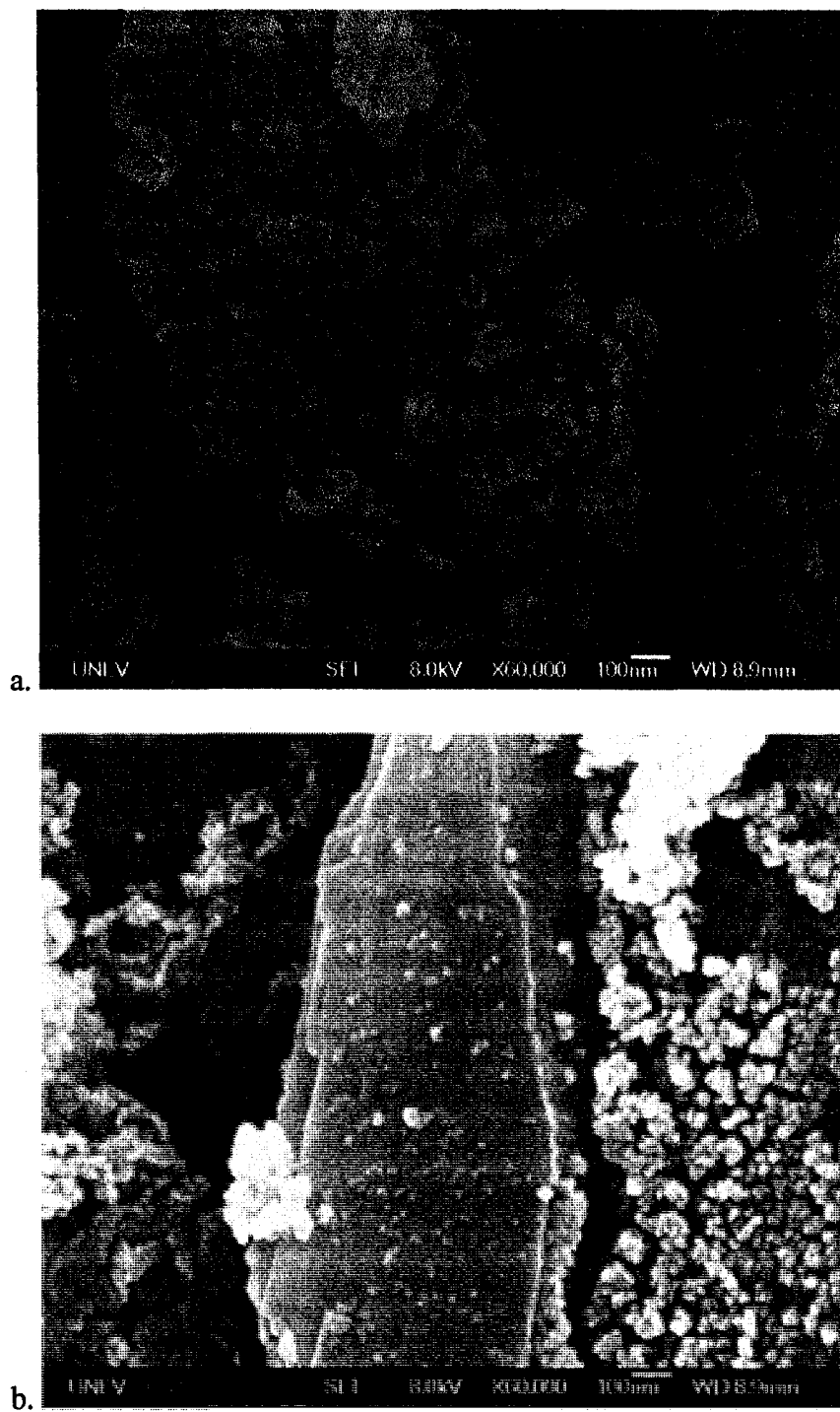


Figure 4.16 SEM images of NaBH_4 reduced Aniline and Palladium complexes a. Aniline/ PdCl_4^{2-} in 0 M HClO_4 b. Aniline/ PdCl_4^{2-} in 1.0 M HClO_4

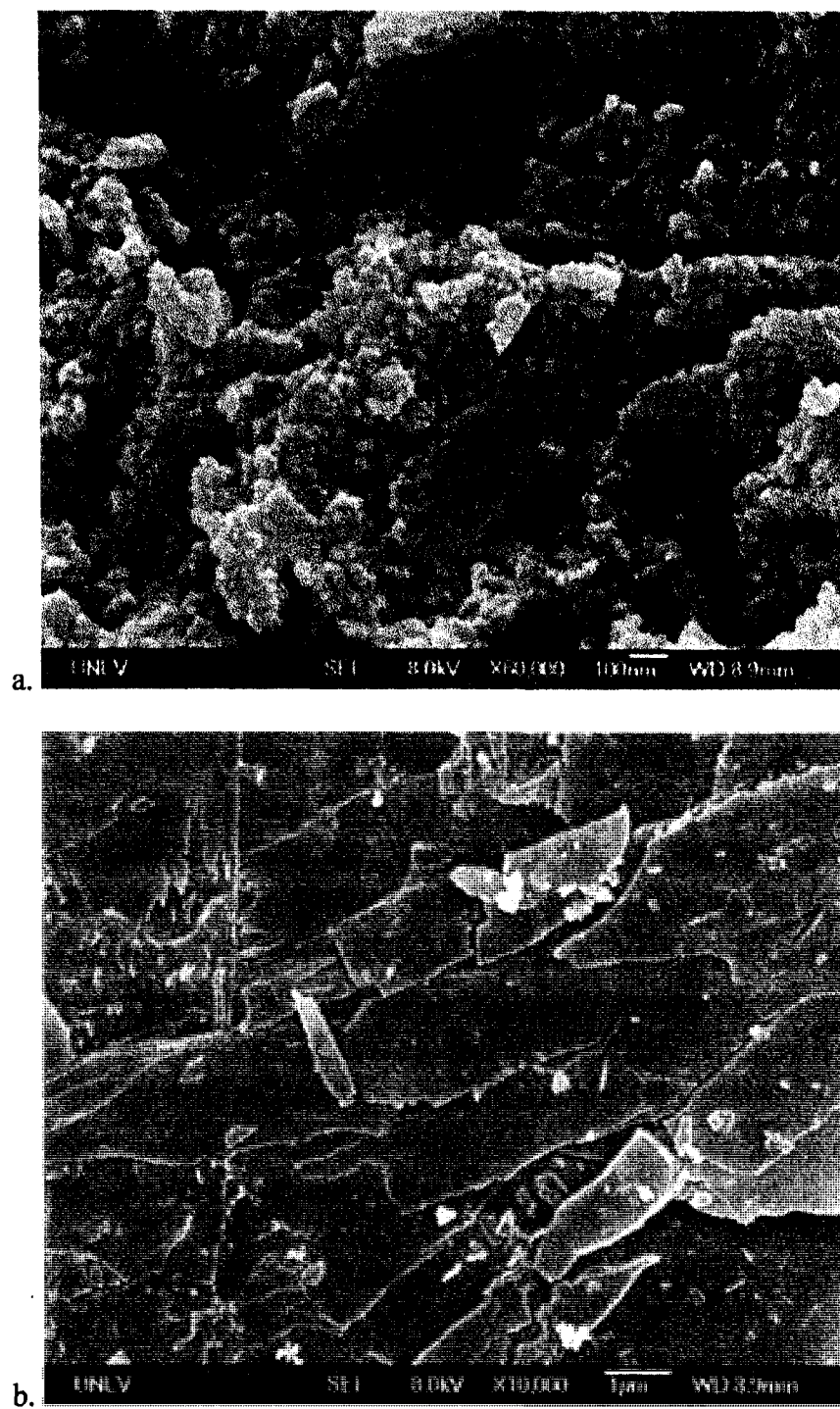


Figure 4.17 SEM images of NaBH_4 reduced Aniline and Palladium complexes a. Aniline/ PdCl_6^{2-} in 0 M HClO_4 b. Aniline/ PdCl_6^{2-} in 1.0 M HClO_4

4.6 Applications

The application of the materials developed will focus on hydrogen sorption rather than the other possible applications, including catalysis and fuel cells. These materials would be applicable to both fields but these studies would exceed the scope of this thesis. The imaging and spectroscopic data concludes that these composites were not fully polymeric in nature and some applications may not be feasible. Applications such as rechargeable batteries require the use of PANI in the emeraldine base form rather than complexes formed from Pd and aniline.¹⁵ Batteries also need a conductive material that can withstand repetitive charging and discharging of current. The eight materials examined thus far do not form pure PANI and have insulating properties inconsistent with the application mentioned. Fortunately, there are applications in which these solids still have potential. Hydrogen storage is one application that does not require the material to have high conductivity, be composed of only polymer, or have a defined structure of morphology consistent with polymer formation.

4.6.1 Introduction to Hydrogen Storage

An in house hydrogen sorption technique was developed to measure low pressure hydrogen sorption of the materials. The experimental setup for these measurements was described in detail in section 2.4. This setup eliminates conditions that would require specialized equipment and precautions due to the hazard of high pressure hydrogen measurements. For our studies, we used a hydrogen generator typically utilized in GC/FID to provide a stream of 30 psi hydrogen at 50 mL/min. Each measurement was carried out with an initial purge of hydrogen gas through the sample for 90 seconds. Samples were then exposed to static hydrogen at 30 psi for increasing periods of times

from 5 to 90 minutes. The samples were placed in line with the GC to measure hydrogen desorption as a function of temperature. The samples were initially held at 35°C for five minutes. The temperature was then ramped to 200°C at a rate of 1.5°C/second to elute the unsorbed and sorbed hydrogen.

It is generally believed that the metallic Pd content is the critical component in the material because Pd hydrides can form. However, we have shown previously using XPS data that the Pd is not metallic. The influence of oxidized Pd on hydrogen sorption properties is unknown. If the material produced sorb hydrogen, then we would expect the amount sorbed to increase with time until all active sorption sites are consumed. In addition, the role of the polymer in the process is unknown. There are conflicting results regarding hydrogen sorption by PANI alone.^{16,17} It has been reported that pure PANI may absorb up to 8% hydrogen by weight with others reporting that as little as 0.5% is sorbed.^{16,17} Therefore, we examined the pure polymer as well as the materials produced in these studies. The goal was to identify materials with favorable hydrogen sorption properties in comparison to PANI. It is important to point out that the pressures employed in these studies are significantly below the pressures used to examine the previous materials. The parameters used in these experiments were carried out at a low pressure of 30 psi compared to the data obtained in the literature at a much higher pressure of 1350 psi outlined in the Department of Energy targets for hydrogen sorption pressures.

4.6.2 Hydrogen Storage of Aniline and Palladium Complexes

Figure 4.18 shows the Aniline/0 M HClO₄ PdCl₄²⁻ material because it had and retained the highest hydrogen storage. Peak (a) represents the hydrogen that was

unabsorbed and (b) represents hydrogen sorbed. The flat line represents the 5 minute sorption time and has no hydrogen storage present. The sorption peaks increase, with 40 minutes being the highest. As expected, the unabsorbed hydrogen peak (a) remained constant over time. This is of importance because a constant concentration of hydrogen is in the column at every interval.

The results are presented in Figure 4.19 for the materials produced using aniline. The plots are for various hydrogen exposure times. The two materials produced using PdCl_4^{2-} show an increase in sorption for exposure time up to 40 minutes. However, the hydrogen sorption decreases after exposure for greater than forty minutes. It is important to state that the plots are for a single sample cycled after different sorption times. For each sorption experiment the sample is exposed to hydrogen at 35°C. To measure the desorption of hydrogen the sample is maintained at 35°C for four minutes to allow the unsorted hydrogen to exit the GC. After five minutes the sample is ramped up to 200°C. This temperature exceeds the threshold for degradation of the material as determined by TGA. Therefore, it can be concluded from the PdCl_4^{2-} data that there is thermal degradation of the material that results in a loss of hydrogen sorption. Therefore, the temperature for the desorption of hydrogen from the materials must be lowered to ensure the composition does not change or the materials must be treated to produce chemically stable material at higher temperature. The aniline prepared materials peak at 40 minutes, except for the 1.0 M HClO_4 PdCl_6^{2-} material, which had insignificant hydrogen storage capacities, compared to the other three. The 0 M HClO_4 PdCl_4^{2-} material retained higher hydrogen storage percentage compared to the others, yet still showed thermal degradation over time.

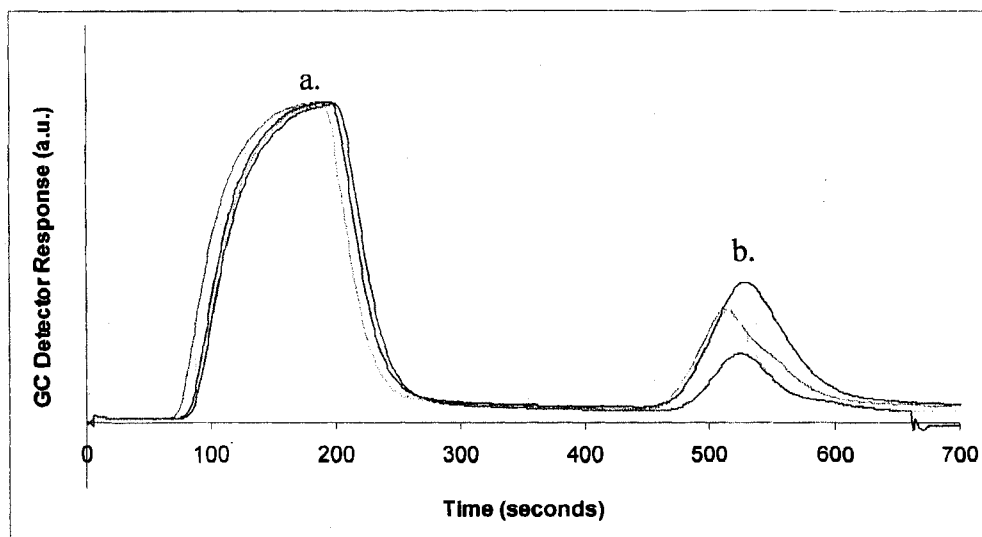


Figure 4.18 Hydrogen Storage of Aniline/0 M HClO_4 PdCl_4^{2-} a. unabsorbed hydrogen b. absorbed hydrogen.

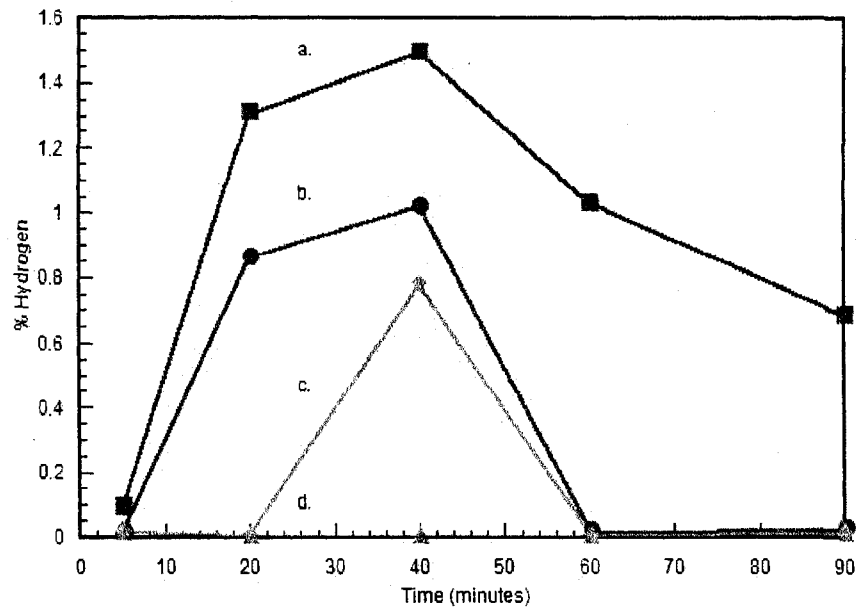


Figure 4.19 Hydrogen Storage of Aniline/Palladium complexes a. 0 M HClO_4 PdCl_4^{2-} b. 1.0 M HClO_4 PdCl_4^{2-} c. 0 M HClO_4 PdCl_6^{2-} d. 1.0 M HClO_4 PdCl_6^{2-}

4.6.3 Hydrogen Storage of NPPD and Palladium Complexes

Figure 4.20 shows NPPD/0 M HClO_4 PdCl_4^{2-} as comparison to the aniline counterpart. Peak (a) represents the hydrogen that was unabsorbed and (b) represents hydrogen sorbed. This graph shows a steady increase of hydrogen sorption over time with a steady value of unabsorbed hydrogen. This material showed hydrogen sorption at the 5 minute point as opposed to the aniline/0 M HClO_4 PdCl_4^{2-} .

The Pd loading data suggested that the aniline/Pd materials should have higher sorption properties relative to materials produced using NPPD. Thermal analysis results indicate that there is a much lower palladium composition than its aniline counterparts. We expect that these materials will have lower sorption properties when compared to aniline based materials due to the lower Pd loading. The one exception was the material produced using PdCl_4^{2-} and 1 M HClO_4 with NPPD with the Pd loading on the order of 20% from TGA analysis. Figure 4.21 shows the sorption characteristics over time for materials produced using NPPD reacted with PdCl_4^{2+} and PdCl_6^{2+} with 0 and 1 M HClO_4 .

In contrast to the materials produced using aniline, there is a steady increase of hydrogen sorption for the materials over the same time range with no loss of sorption. The data implies that materials produced using NPPD have higher thermal stability. The PdCl_6^{2+} solids reach a plateau after 60 minutes indicating that its hydrogen capacity had been reached.

The NPPD/ Pd^{2+} materials had higher hydrogen sorption properties and steadily increased over time. The 1.0 M HClO_4 PdCl_4^{2-} material had the highest increase in hydrogen sorption and showed high sorption at only 5 minutes. The 0 M HClO_4 PdCl_4^{2-} material showed a steady increase of sorption over time. The NPPD/ Pd^{4+} materials both

had peak hydrogen sorption at 60 minutes. The 90 minute time points for 0 M HClO_4 PdCl_6^{2-} and 1.0 M HClO_4 PdCl_6^{2-} were almost identical to the 40 minute run.

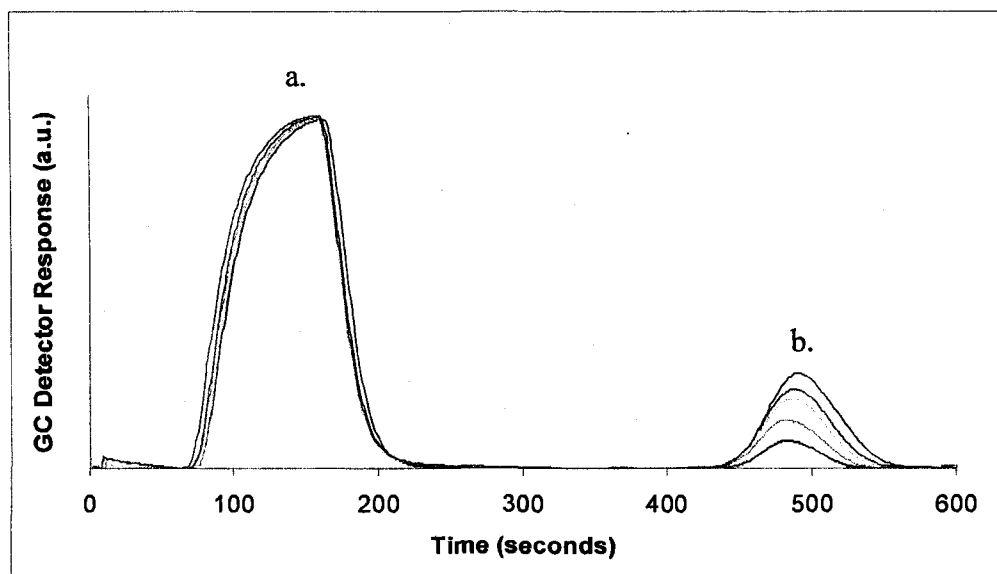


Figure 4.20 Hydrogen Storage of NPPD/0 M HClO_4 PdCl_4^{2-} a. unabsorbed hydrogen b. absorbed hydrogen.

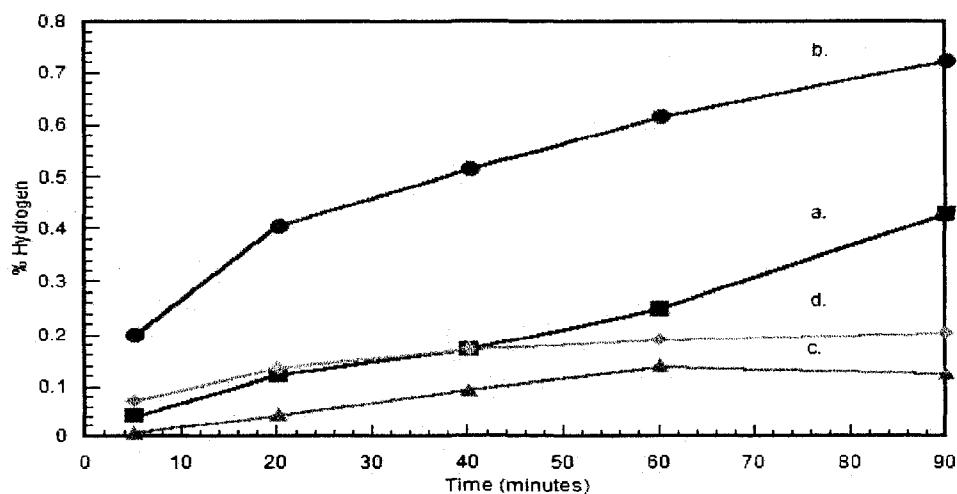


Figure 4.21 Hydrogen Storage of NPPD/Palladium complexes a. 1.0 M HClO_4 PdCl_4^{2-} b. 1.0 M HClO_4 PdCl_6^{2-} c. 0 M HClO_4 PdCl_6^{2-} d. 1.0 M HClO_4 PdCl_6^{2-}

4.6.4 Hydrogen Storage of NaBH₄ Treated Aniline/Palladium Material

The 0 M HClO₄ PdCl₄²⁻ Aniline material was treated with NaBH₄ to determine whether reducing the materials would show an increase in hydrogen sorption. Figure 4.22 shows the NaBH₄ treated sample with all the aniline prepared materials for comparison. Immediately, at five minutes, hydrogen sorption jumps from 0.1% to 1.7%. Also, the treated material maintained hydrogen sorption over repetitive cycling.

Even though this is preliminary data, it can be concluded that NaBH₄ treatment may stabilize and reduce the complex. Thermal degradation is not a problem after repetitive thermal cycling making the 0 M HClO₄ PdCl₄²⁻ Aniline prepared material better suited for hydrogen storage applications.

4.7 Conclusion

Overall, the aniline prepared materials sorbed a higher percentage of hydrogen compared to NPPD. At approximately 1.5%, 0 M HClO₄ PdCl₄²⁻ was the highest absorbing material. The aniline materials displayed characteristics of thermal degradation from the drops in hydrogen sorption over time. The NPPD solids showed a stable increase of hydrogen sorption over time.

In comparing oxidation state of palladium, PdCl₄²⁻ and PdCl₆²⁻, the Pd²⁺ complexes showed the highest sorption characteristics than Pd⁴⁺. This may be attributed to the possibility of Pd²⁺ reducing to Pd metal quicker than Pd⁴⁺.

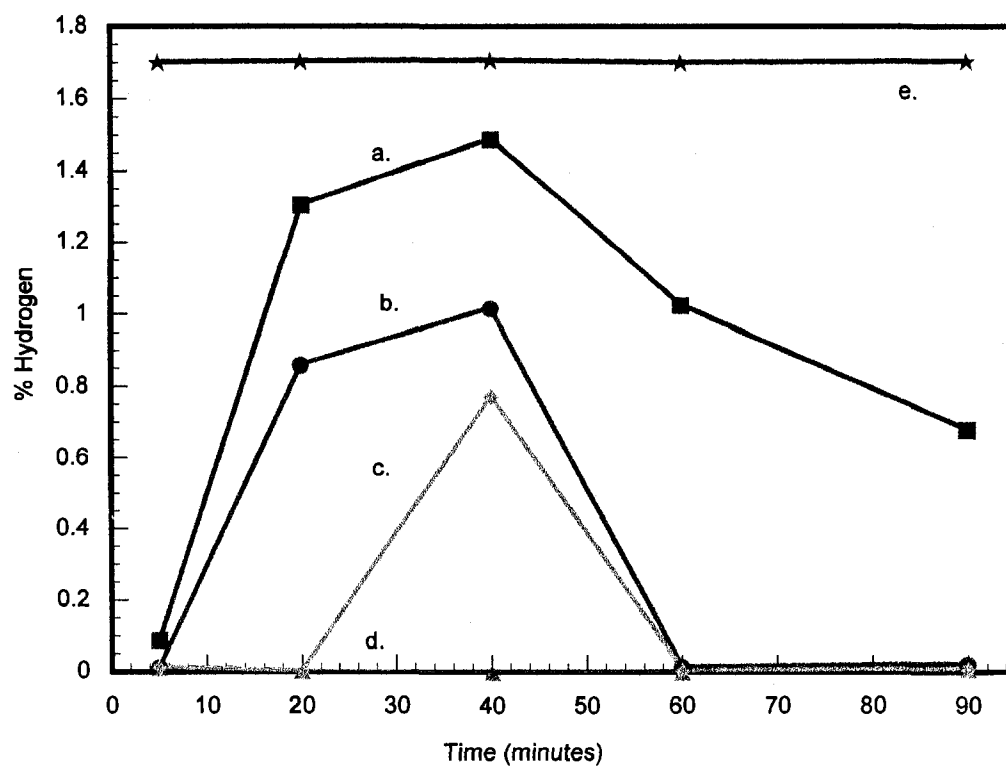


Figure 4.22 Hydrogen Storage of Aniline/Palladium complexes a. 0 M HClO_4 PdCl_4^{2-} b. 1.0 M HClO_4 PdCl_4^{2-} c. 0 M HClO_4 PdCl_6^{2-} d. 1.0 M HClO_4 PdCl_6^{2-} e. NaBH_4 treated 0 M HClO_4 PdCl_4^{2-}

4.8 References

- (1) Palaniappan, S. *Polymers for Advanced Technologies* **2002**, *13*, 54-59.
- (2) Wei, Y.; Hsueh, K. F. *Journal of Polymer Science, Part A: Polymer Chemistry* **1989**, *27*, 4351-4363.
- (3) Chandrakanthi, N.; Careem, M. A. *Polymer Bulletin* **2000**, *44*, 101-108.
- (4) Chen, C.-H. *Journal of Applied Polymer Science* **2003**, *89*, 2142-2148.
- (5) Traore, M. K.; Stevenson, W. T. K.; McCormick, B. J.; Dorey, R. C.; Wen, S.; Meyers, D. *Synthetic Metals* **1991**, *40*, 137-153.
- (6) Syed, A. D., Maravattickal K. *Talanta* **1991**, *28*, 815-837.
- (7) Kinyanjui, J. M.; Wijeratne, N. R.; Hanks, J.; Hatchett, D. W. *Electrochimica Acta* **2006**, *51*, 2825-2835.
- (8) Xu, J. C.; Liu, W. M.; Li, H. L. *Materials Science and Engineering C* **2005**, *25*, 444-447.
- (9) Hatchett, D. W.; Josowicz, M.; Janata, J. *Journal of Physical Chemistry B* **1999**, *103*, 10992-10998.
- (10) Pan, Y. L.; Zhao, F.; Yang, S. *Acta Crystallographica Section E: Structure Reports Online* **2006**, *62*, m239-m240.
- (11) Biáek, B. *Surface Science* **2006**, *600*, 1679-1683.
- (12) Mallick, K.; Witcomb, M.; Scurrrell, M. *Platinum Metals Review* **2007**, *51*, 3-15.
- (13) Wagner, C. D., Riggs, W. M., Davis, L. E., Moulder, J. F., and G. E. Muilenberg *Handbook of X-Ray Photoelectron Spectroscopy*; Perkin-Elmer Corporation: Eden Prairie, Minnesota, 1979.

- (14) Stejskal, J.; Hlavata, D.; Holler, P.; Trchova, M.; Prokes, J.; Sapurina, I. *Polymer International* **2004**, 53, 294-300.
- (15) Macdiarmid, A. G.; Yang, L. S.; Huang, W. S.; Humphrey, B. D. *Synthetic Metals* **1986**, 18, 393-398.
- (16) Cho, S. J.; Song, K. S.; Kim, J. W.; Kim, T. H.; Choo, K. In *ACS Division of Fuel Chemistry, Preprints*; 2 ed. 2002; Vol. 47, p 790-791.
- (17) Panella, B.; Kossykh, L.; Dettlaff-Weglikowska, U.; Hirscher, M.; Zerbi, G.; Roth, S. *Synthetic Metals* **2005**, 151, 208-210.

CHAPTER 5

CONCLUSION

5.1 Conclusion

The goal of this research was to chemically synthesize and characterize materials produced from either aniline or NPPD with the addition of either PdCl_4^{2-} or PdCl_6^{2-} with or without HClO_4 . These materials were synthesized for their potential use in hydrogen storage. All eight of these materials have been characterized and tested for their hydrogen sorption characteristics. The results of these studies have been discussed in this thesis.

It has been shown that using PdCl_4^{2-} or PdCl_6^{2-} as the chemical oxidant for the formation of polymer was not successful. Instead, the materials were mixtures of complex and low molecular weight oligomers. In the case of the NPPD prepared materials, the NPPD/ Pd^{4+} composites showed slight polymer formation that was displayed in their corresponding IR spectra. No polymer formation was observed for the aniline/Pd composites. TG results indicated that even though the NPPD analog produced polymer when reacted with PdCl_4^{2-} or PdCl_6^{2-} as the chemical oxidant, the materials had lower total palladium content than the aniline counterparts. NPPD materials had a maximum of 11% Pd content, whereas the maximum aniline/Pd content was 27%.

The SEM images show that the composites are not conductive PANI. The formation of complexes may account for the final oxidation state of the incorporated Pd. The XPS results demonstrate that the Pd remains oxidized in the materials.

Preliminary hydrogen storage studies showed that materials with PdCl_4^{2-} had higher storage capacities than the PdCl_6^{2-} materials. Also, the aniline/Pd complexes were undergoing thermal degradation at 200°C . The NPPD/Pd materials retained structural integrity and in turn showed a steady and stable increase in hydrogen sorption over time. There were three promising samples; Aniline/0 M HClO_4 PdCl_4^{2-} , Aniline/1.0 M HClO_4 PdCl_4^{2-} , and NPPD/1.0 M HClO_4 PdCl_4^{2-} . These three materials showed the highest hydrogen sorption properties.

Further research was done to chemically reduce Pd to its metallic state in the composites using NaBH_4 . Only Aniline/0 M HClO_4 PdCl_4^{2-} was analyzed by the GC. Hydrogen sorption instrument and was the highest out of all previous eight materials at 1.8%. Further studies need to be done in order to determine the magnitude of the sorption properties for all reduced materials.

VITA

Graduate College
University of Nevada, Las Vegas

Jade L. Morgan

Home Address:

808 Bonita Ave
Las Vegas, NV 89104

Degrees:

Bachelor of Science, Biochemistry, 2005
University of Nevada, Las Vegas

Thesis Title: Synthesis and Characterization of Aniline Based Palladium Composites and Complexes

Thesis Examination Committee:

Chairperson, Dr. David W. Hatchett, Ph.D.
Committee Member, Dr. Spencer Steinberg, Ph.D.
Committee Member, Dr. Ken Czerwinski, Ph.D.
Graduate Faculty Representative, Dr. Jacimaria Batista, Ph.D.